energies

MDPI

Review

A Review of Reliability Assessment and Lifetime Prediction Methods for Electrical Machine Insulation Under Thermal Aging

Jian Zhang [1,2], Jiajin Wang [1,2], Hongbo Li [3], Qin Zhang [1,2], Xiangning He [1,2], Cui Meng [2], Xiaoyan Huang [2], Youtong Fang [2] and Jianwei Wu [4,*]

[1] State Key Laboratory of Fluid Power and Mechatronic Systems, Zhejiang University, Hangzhou 310027, China
[2] College of Electrical Engineering, Zhejiang University, Hangzhou 310027, China
[3] Zhejiang Guoli Security Technology Co., Ltd., Hangzhou 310053, China
[4] School of Mechanical Engineering, Zhejiang University, Hangzhou 310027, China
* Correspondence: sdwjw@zju.edu.cn

Abstract: The thermal aging of insulation systems in electrical machines is a critical factor influencing their reliability and lifetime, particularly in modern high-performance electrical equipment. However, evaluating and predicting insulation lifetime under thermal aging poses significant challenges due to the complex aging mechanisms. Thermal aging not only leads to the degradation of macroscopic properties such as dielectric strength and breakdown voltage but also causes progressive changes in the microstructure, making the correlation between aging stress and aging indicators fundamental for lifetime evaluation and prediction. This review first summarizes the performance indicators reflecting insulation thermal aging. Subsequently, it systematically reviews current methods for reliability assessment and lifetime prediction in the thermal aging process of electrical machine insulation, with a focus on the application of different modeling approaches such as physics-of-failure (PoF) models, data-driven models, and stochastic process models in insulation lifetime modeling. The theoretical foundations, modeling processes, advantages, and limitations of each method are discussed. In particular, PoF-based models provide an in-depth understanding of degradation mechanisms to predict lifetime, but the major challenge remains in dealing with complex failure mechanisms that are not well understood. Data-driven methods, such as artificial intelligence or curve-fitting techniques, offer precise predictions of complex nonlinear relationships. However, their dependence on high-quality data and the lack of interpretability remain limiting factors. Stochastic process models, based on Wiener or Gamma processes, exhibit clear advantages in addressing the randomness and uncertainty in degradation processes, but their applicability in real-world complex operating conditions requires further research and validation. Furthermore, the potential applications of thermal lifetime models, such as electrical machine design optimization, fault prognosis, health management, and standard development are reviewed. Finally, future research directions are proposed, highlighting opportunities for breakthroughs in model coupling, multi-physical field analysis, and digital twin technology. These insights aim to provide a scientific basis for insulation reliability studies and lay the groundwork for developing efficient lifetime prediction tools.

Keywords: thermal aging; physics of failure; artificial intelligence algorithms; curve-fitting technologies; stochastic process; application of insulation lifetime model

Academic Editor: José Matas

Received: 30 December 2024
Revised: 22 January 2025
Accepted: 24 January 2025
Published: 25 January 2025

Citation: Zhang, J.; Wang, J.; Li, H.; Zhang, Q.; He, X.; Meng, C.; Huang, X.; Fang, Y.; Wu, J. A Review of Reliability Assessment and Lifetime Prediction Methods for Electrical Machine Insulation Under Thermal Aging. *Energies* **2025**, *18*, 576. https://doi.org/10.3390/en18030576

1. Introduction

The reliability and lifetime of electrical machines (EMs) are critical to the effective operation of various industrial and commercial systems. At the core of these attributes is the electrical insulation system (EIS), which plays a crucial role in maintaining the electrical integrity and mechanical robustness of these machines. The EIS of EM acts as a barrier to prevent leakage and short circuits, ensuring the safe and reliable operation of the equipment. However, in modern high-performance electrical devices, these machines operate under highly variable and often harsh conditions, exposing the EIS to a range of stress factors, such as thermal, electrical, environmental, and mechanical stresses, collectively referred to as TEAM stresses [1]. Among these, thermal stress arises from external environmental conditions and the internal heat generated during operation. Prolonged exposure to high temperatures accelerates the degradation of materials within the EIS, ultimately leading to performance deterioration and premature failure. Although other stress factors, such as electrical surges or mechanical vibrations, can also contribute to aging, their impacts are typically intermittent or secondary [2]. To address the risks posed by electrical stress, manufacturers often incorporate corona-resistant (CR) materials into the insulation, allowing the insulation to continue functioning even when exposed to partial-discharge risks. Mechanical stress induced by vibration can cause the enamel layer to become brittle, potentially leading to detachment [3]. A viable solution is to employ varnish impregnation as a preventive measure during the design and manufacturing stages of EMs. Furthermore, while many insulation materials are hygroscopic, humidity itself does not significantly contribute to aging when analyzing conventionally dry-immersed motors [2,4]. In contrast, thermal stress exerts a continuous influence, making it the primary factor that accelerates insulation degradation and limits the lifetime of the motor. Over-engineering with thicker, higher thermal-grade insulation materials can provide sufficient safety margins, but this approach conflicts with the design requirements for high-power-density motors [5]. Therefore, understanding the behavior of insulation under thermal stress is crucial for predicting the operational lifetime of motors and maintaining their performance.

Thermal aging is a complex process involving a series of chemical and physical changes within insulation materials. These changes manifest as degradation of macroscopic electrical performance parameters and gradual alterations in the microscopic structure, such as a loss of dielectric strength, reduction in breakdown voltage, darkening of color, changes in texture, and the formation of microcracks and voids. From a macroscopic perspective, thermal aging leads to a significant decline in key indicators such as insulation strength, insulation resistance, and breakdown voltage, severely impairing dielectric, thermal, and mechanical properties, which can lead to premature insulation failure [6–9]. At the microscopic level, thermal stress induces oxidation, depolymerization, and the chain breakage of the polymers within the insulation, altering the material's morphology and resulting in the formation of voids, surface erosion, and embrittlement. For instance, thermal aging can cause polymer chain crosslinking, reducing flexibility and increasing brittleness. Additionally, the formation of microcracks and voids compromises the structural integrity of the insulation material. Thermal aging leads to irreversible oxidation reactions, the progress of which directly reflects the degree of insulation degradation [10]. A typical schematic diagram of thermal oxidation aging in epoxy resin is shown in Figure 1 [11]. Numerous studies have demonstrated that, as oxidation progresses, the quality of the insulation material deteriorates [12], chemical functional groups change [13], the microscopic structure becomes more complex [14,15], and the degree of microscopic carbonization increases [16]. Theoretically, these microscopic characteristics can all serve as reliable indicators of insulation aging. It is important to note that these microscopic structural defects

are often considered the initiation points of macroscopic failure. Furthermore, thermal aging accelerates the physical and chemical transformations in composite EIS. For example, delamination between layers, the cracking of filler materials, and the mismatch of thermal expansion between different components exacerbate degradation [5]. These issues are more complicated in high-performance motors, where compact designs and high power densities amplify thermal stress, making insulation thermal failure a major concern. An increase in temperature accelerates the aging process, resulting in a significant reduction in the lifetime of winding insulation. According to general experience, a 10 °C rise in temperature corresponds to a 50% reduction in insulation lifetime [3].

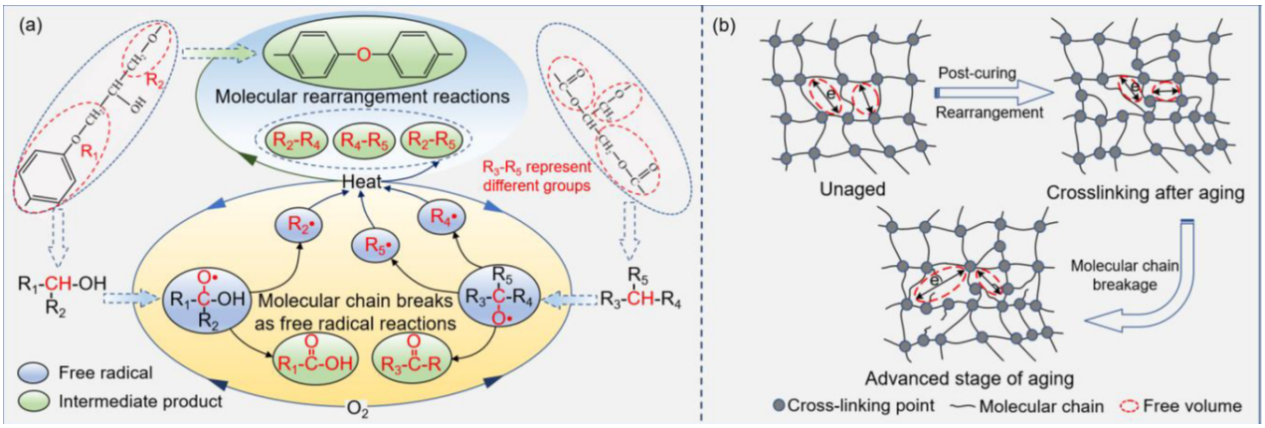

Figure 1. A schematic diagram of the thermo-oxidative aging process of epoxy resin. (**a**) Thermo-oxidation aging process. (**b**) Changes in the crosslinked structure [11].

The critical role of the EIS and the widespread impact of thermal stress highlight the necessity of developing reliable models to predict insulation lifetime under thermal aging. Accurate lifetime prediction models offer numerous benefits. They enable precise predictions of insulation lifetime, minimizing downtime and preventing catastrophic events. In addition, these models provide deep insights into the degradation trajectories of insulation materials, thus optimizing maintenance schedules and reducing operational costs. Beyond operational improvements, the lifetime models developed inform the design of more resilient, reliability-oriented electrical machines, ultimately enhancing the reliability and performance of the machines. However, since insulation is a typical high-reliability, long-lifetime product, it is challenging to obtain sufficient failure or degradation data over a short period to derive a lifetime distribution [17]. Accelerated lifetime tests (ALTs) and accelerated degradation tests (ADTs) allow the insulation failure process to be expedited under higher stress levels, generating more comprehensive data in a shorter time frame to establish lifetime models. Current research on insulation lifetime modeling can generally be categorized into three approaches: physics of failure (PoF), data-driven, and degradation process-based models. PoF models delve into the fundamental mechanisms of insulation aging, often incorporating material-specific characteristics and thermally activated processes (see Section 3 for a detailed discussion). Data-driven techniques, which utilize statistical tools and artificial intelligence (AI) algorithms, focus on pattern recognition in lifetime or degradation data, providing predictive capabilities without relying on explicit failure mechanisms (see Section 4 for a detailed discussion). Degradation process-based frameworks, such as stochastic models and cumulative damage theory, bridge the gap between physics-based insights and empirical observations by modeling aging as a probabilistic process influenced by stress factors (see Section 5 for a detailed discussion). Developing advanced lifetime prediction models requires a multidisciplinary approach that combines experimental research with computational modeling. These efforts will not

only enhance the reliability of EMs but also make it possible to transition to high-efficiency, high-power-density designs capable of withstanding harsh operating conditions.

This paper aims to systematically review and summarize the methods for reliability assessment and lifetime prediction of EIS under thermal aging, focusing on analyzing the theoretical foundations, modeling processes, advantages, and limitations of different modeling approaches. Furthermore, potential applications in machine design, operation and maintenance, and standard formulation are discussed. Specifically, the structure of the paper is arranged as follows: Section 2 introduces the basic theory of thermal aging in EIS and the impact of thermal stress on insulation performance. In this section, two different thermal failure modes—constant and variable thermal stress, and the experimental designs for these modes—are discussed. Additionally, key aging indicators, covering both macro and micro aspects, are summarized to characterize insulation performance under thermal stress. Section 3 provides a detailed discussion of insulation lifetime modeling based on PoF, primarily focusing on the theoretical framework of these models, lifetime modeling under constant and variable temperatures, and their application cases in engineering practice. Section 4 explores data-driven insulation lifetime modeling methods, with an emphasis on the application of AI algorithms and curve-fitting (CF) techniques in characterizing degradation trends and predicting lifetime. The advantages, disadvantages, and practical application potential of these methods are analyzed. Section 5 introduces insulation lifetime prediction methods based on stochastic processes, discussing the applications of Wiener process and Gamma process in thermal aging modeling, particularly in degradation processes with strong uncertainty and randomness. Section 6 discusses the practical applications of thermal lifetime models, including potential uses in machine design optimization, fault prediction, and health management, as well as standard formulation and testing method improvements. Finally, Section 7 concludes the review, proposes future research directions, and forecasts the further development of thermal lifetime models in intelligent machine systems.

2. Insulation Accelerated Tests and Aging Indicators Under Thermal Stress

Thermal aging is a long-term process, and its impact on the probability of insulation failure may not become apparent until after extended operation. Therefore, ALTs and ADTs are typically used to gather data and ultimately determine the insulation's lifetime and quality statement within a reasonable framework. This section summarizes the research on insulation aging under constant and variable thermal stresses and identifies commonly used aging indicators that have been proven effective.

2.1. Insulation Aging Under Constant Thermal Stress

The expected lifetime of insulation at the highest temperature permitted by the its thermal class is 20,000 h, which is a very time-consuming and impractical test. The IEC 60034-18-21 standard acknowledges this limitation and recommends conducting ADTs at three or more higher temperatures [18]. Giangrande et al. [2] performed accelerated thermal aging tests on motor coils rated for a thermal class of 200, at temperatures of 230 °C, 250 °C, and 270 °C, with high-precision ventilated ovens controlling the temperature error within 1 °C. The duration of each thermal aging cycle depends on the chosen aging temperature and follows the test procedure summarized in the flowchart in Figure 2. After each aging cycle, the samples were naturally cooled to room temperature for insulation diagnostic testing to evaluate their condition. Hi-pot testing was used to assess the dielectric strength of the aged samples, which served as the failure criteria for the aging specimens. The failure time of the failed samples was recorded, while the remaining samples continued to age until

all samples failed or reached the predetermined aging cycle. After the tests, the collected data were processed and analyzed to establish the lifetime model. Khowja et al. [19] provided an accelerated thermal aging test platform for twisted pairs, which mainly consists of an oven and insulation diagnostic equipment, as shown in Figure 3. The Megger 4110 is used to apply a 0–700 V, 50 Hz AC voltage to the insulation specimen, measuring diagnostic parameters such as tanδ and IC at the end of each aging cycle, and ultimately monitoring the insulation breakdown. The dissipation factor measurement ranges from 0% to 10000% with 0.001% maximum resolution and the capacitance measurement ranges from 0 to 100 µF with 0.01 pF maximum resolution. Further descriptions of insulation aging under constant thermal stress can also be found in [17,20–22], where similar approaches were used to design thermal aging tests, although differences exist in the selection of aging temperatures, aging cycles, and monitoring indicators, as the specimens studied were not identical.

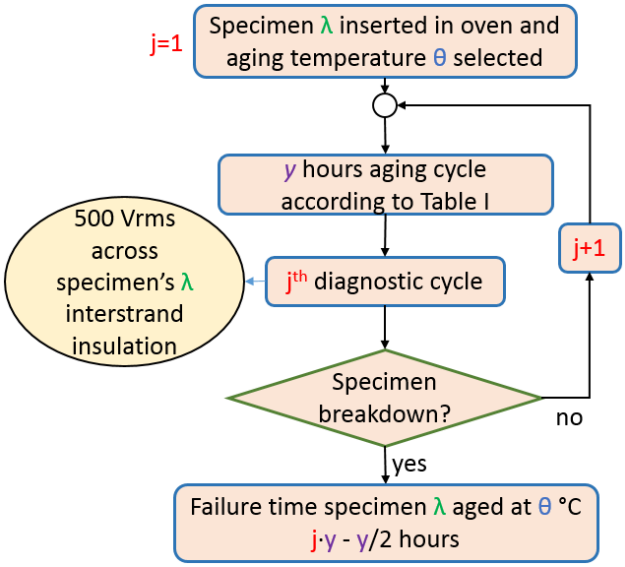

Figure 2. A flowchart of the accelerated thermal aging tests [2].

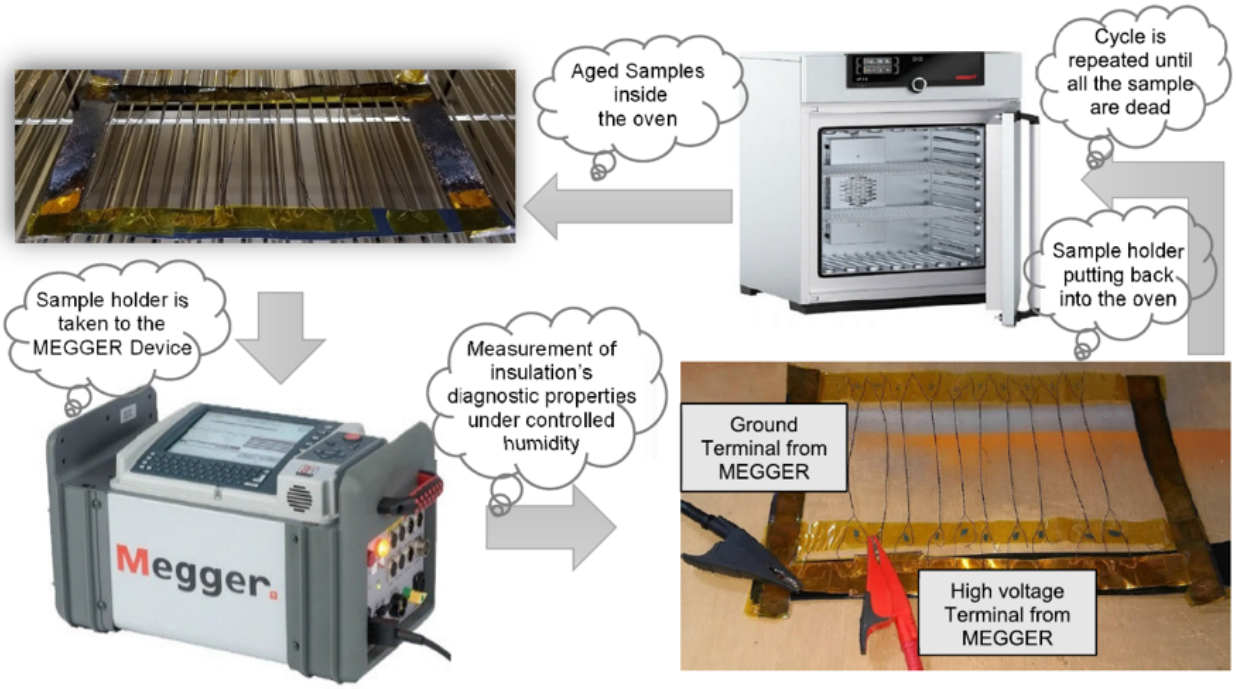

Figure 3. Measurement setup for accelerated aging tests [19].

2.2. Insulation Aging Under Variable Thermal Stress

In actual operating conditions, EIS often experiences periodic temperature fluctuations. The impact of such variable thermal stress on insulation degradation is significantly different from that of constant thermal stress. It is generally believed that temperature variations cause materials to expand and contract, with different materials exhibiting varying thermal expansion coefficients [23,24]. IEC and IEEE technical standards also point out that the effects of thermal cycling on insulation life cannot be ignored, especially in high-power-density motors [25,26].

Kokko et al. [27] proposed a method for predicting the thermal cycling aging of hydrogenerator stator windings caused by start–stop cycles. They applied a multi-physics coupled model to calculate the residual life of stator windings and matched model parameters with a database of different insulation systems and generators. Their findings presented the lifetime consumption hours for asphalt–mica and epoxy–mica winding insulation systems and recommended simultaneous electrical and thermal cycling tests under high characteristic electric-field stresses. Mitsui et al. [28] conducted an in-depth study of thermal cycling degradation in epoxy–mica insulation used in AC high-voltage motors. The experiments revealed that insulation degradation begins with separation between the groundwall insulation (GI) layer and the strand insulation at the iron core ends. This degradation spreads through delamination and crack formation in the mica layers. The study emphasized the importance of compatibility between strand insulation and GI in mitigating thermal cycling degradation and advocated for thermal cycling tests under voltage stress to more accurately capture the degradation behavior of actual EMs. Madonna et al. [3] investigated the insulation aging characteristics of EMs operating under short duty cycles through cyclic temperature tests. The study focused on random-wound coils and designed multiple temperature cycling profiles, applying thermal stress within a temperature range exceeding the thermal rating of the insulation. The test results showed that temperature cycling significantly accelerated the insulation aging process, with the insulation lifetime halving for every 7 °C increase in temperature. This approach revealed the dynamic effects of cyclic thermal stress on insulation performance, surpassing the limitations of traditional constant-temperature models and providing new insights into reliability assessment and design for short-cycle operating equipment such as aerospace motors. Building on this, Zhou et al. [29] analyzed the effects of different temperature cycling profiles on the insulation lifetime of low-voltage motors by comparing accelerated lifetime tests under constant and variable temperature conditions. The tests included three temperature profiles, covering different combinations of maximum and minimum temperatures (220 °C–260 °C, 230 °C–270 °C, 240 °C–280 °C) while maintaining the same temperature gradient and cycle period. The temperature profile curves in the tests are shown in Figure 4. A statistical analysis of experimental data using Weibull distribution demonstrated that under the same maximum temperature conditions, the lifetime loss caused by cyclic temperature aging was significantly higher than that of constant-temperature aging. The results verified that cyclic thermal stress introduces additional thermal–mechanical stress. Furthermore, the authors constructed an Arrhenius–Miner lifetime model to quantitatively analyze the additional lifetime loss and proposed the concept of equivalent experimental and theoretical temperatures. This concept provides new theoretical tools and experimental evidence for evaluating insulation lifetime under variable temperature conditions.

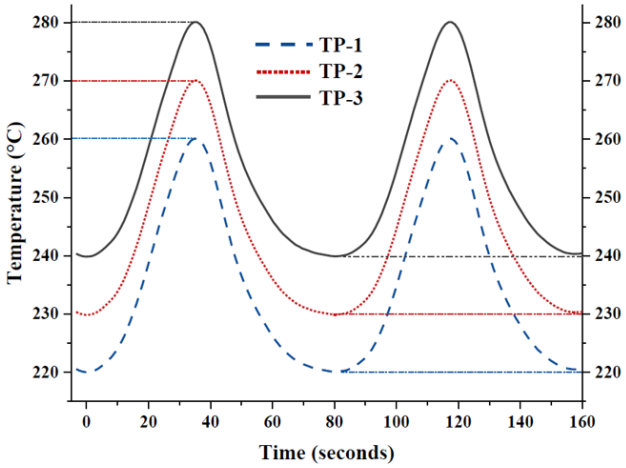

Figure 4. Variable temperature profiles for experiments in the literature [29].

2.3. Macroscopic Aging Indicators

Selecting appropriate insulation performance characterization parameters as aging indicators is the first challenge to address when constructing insulation condition estimation and lifetime prediction models. An ideal performance characterization parameter should meet the following three criteria: it must be measurable online, quantifiable, and strongly correlated with insulation lifetime. Insulation performance characterization parameters are typically divided into two categories based on their attributes: macroscopic electrical parameters and microscopic feature parameters. Macroscopic electrical parameters are generally easier to measure and quantify, making them frequently used in industrial applications for real-time monitoring of motor insulation conditions. On the other hand, microscopic feature parameters, due to their difficulty in measurement and quantification, are primarily used for analyzing insulation degradation mechanisms and have not yet been widely applied in the field of lifetime prediction. This subsection provides a review of the current research on motor insulation performance characterization parameters from a macroscopic perspective, analyzing the features and suitable application scenarios of various characterization parameters.

With the advancement of insulation diagnostic testing technologies, mature parameters for characterizing insulation performance have been developed. These parameters primarily include breakdown voltage (BV), insulation resistance (IR), polarization index, dielectric loss, partial discharge (PD), and some derivative parameters. Among these macroscopic electrical parameters, residual breakdown voltage (RBV) is considered particularly unique. It is generally accepted that the lifetime of GI is primarily determined by its RBV, which serves as a reliable indicator of the electrical performance of insulation. According to the IEC, the end of lifetime for GI is defined when the RBV decreases to 50% of its initial value [30]. Unlike general macroscopic electrical parameters, RBV can only be obtained through breakdown testing, a destructive process that irreversibly damages the GI, directly leading to insulation failure and causing the electrical machine to cease operation [6,23]. Consequently, RBV is categorized as a destructive characterization parameter and is typically employed during the factory design stage of GI. It is challenging to use this parameter directly for assessing the remaining lifetime of the GI in operating EMs [23]. Given that RBV is difficult to measure in situ but strongly correlated with the electrical performance of GI, research on evaluating the remaining lifetime of insulation has focused on identifying non-destructive parameters. By establishing relationships between these non-destructive parameters and RBV, the RBV level can be estimated, thereby enabling an understanding of the aging condition of the GI [22].

For medium- and high-voltage electrical machines equipped with Type II insulation materials (organic–inorganic hybrid materials), non-destructive testing equipment has been employed to determine the aging state of the insulation. These techniques include both online monitoring and offline methods [23,31]. Dissipation factor measurements are widely applied in EMs to evaluate the overall condition of insulation [32–34]. For low-voltage machines with Type I insulation materials (organic materials), non-destructive monitoring methods involve measurements of IR, insulation capacitance (IC), and partial discharge-related parameters [21,23,35–38]. In general, these indicators are used to assess the aging condition of the insulation systems in electrical machines. Regarding thermal aging, nearly all studies have reported a decrease in IR and partial-discharge inception voltage (PDIV) during the aging process, while the dielectric dissipation factor (i.e., tanδ) tends to increase. However, conflicting conclusions have been drawn concerning the trend of IC in the literature, and no clear pattern has been established. Cavallini et al. [39] investigated the IC and PDIV of twisted pairs made from enameled wires with a thermal rating of 180 °C, a diameter of 1 mm, and a varnish thickness of 79 µm, manufactured according to IEC standards. These twisted pairs were thermally aged at 230 °C, with each aging cycle lasting 48 h. Testing was conducted after each cycle, and the results showed a continuous decline in both IC and PDIV over time. Wang et al. [40] extensively studied the effects of temperature on PD characteristics and insulation durability, revealing that higher temperatures led to higher PD magnitudes and shorter lifetime. Rumi et al. [41] provided PDIV data for insulation with a thermal class of 200 °C after aging at 230 °C for 28 days. A sharp decline in PDIV was observed after 7 days of aging, followed by a gradual stabilization. After 28 days of aging, the enamel of the twisted pairs became extremely brittle. Differences in PDIV measurements using AC power frequency voltage and pulse voltage were also summarized, showing that while pulse voltage measurements yielded higher initial PDIV, the decline rate was faster. Ji et al. [42] measured the PDIV and partial-discharge extinction voltage (PDEV) of rectangular conductor samples at temperatures ranging from room temperature to the winding's thermal class (180 °C). Samples included those unaged and those thermally aged at 250°C for varying durations (24, 48, 72, and 96 h). The results indicated that both PDIV and PDEV decreased with increasing temperature and thermal aging duration. Naderiallaf et al. [43] studied the PDIV of rectangular coil inter-turn insulation under thermal aging. After aging at 250 °C for 312 h, the average PDIV and the 10th percentile decreased by 17.4% and 21.5%, respectively, which was most likely due to the reduction in insulation thickness during the accelerated thermal aging process. Madonna et al. [44] evaluated the impact of thermal aging on windings used in motors with short duty cycles. Accelerated aging tests were used to study the effects on IC and tanδ. When the applied voltage was below PDIV, IC increased proportionally with aging, and tanδ was unaffected by the thermal aging of the varnish. However, when the applied voltage exceeded PDIV, both IC and tanδ increased with aging time. Savin et al. [38] conducted thermal aging tests on motor winding wires with three different diameters (0.85 mm, 0.95 mm, and 1.25 mm). Samples of two different varnish grades were tested for each diameter. The results showed significant increases in IC and decreases in PDIV across all samples, suggesting these parameters as indicators for inter-turn insulation aging. Madonna et al. [21] proposed a rapid evaluation method for the lifetime of low-voltage motor insulation using thermal aging tests. By selecting IC and its derivative percentage difference ΔIC as aging diagnostic indicators, the degradation of insulation performance during thermal aging was accurately characterized. Experimental verification demonstrated a monotonic increase in ΔIC with aging time, directly correlating with physical changes in varnish thickness. This method significantly reduced the time required for thermal aging tests and provided crucial support for modeling thermal lifetime and reliability assessment of low-voltage motor insulation

systems. Zhe et al. [45] investigated the aging mechanism and lifetime models of electric vehicle motor insulation, proposing that aging is caused by high average temperatures and temperature cycling. The results showed that IC exhibited a more consistent decline during aging compared to IR under various thermal stress levels. Reductions of 4–6% and 11–12% were observed for inter-winding and winding-to-ground capacitance, respectively. Gyftakis et al. [46] analyzed the dielectric properties of PAI insulation used in coated copper wires. Tests on unaged and thermally aged samples revealed reductions in IC and IR over aging time. The decrease in IR was less significant than that of IC. Farahani et al. [47] measured the dissipation factor, IR, and partial-discharge characteristics after each thermal aging cycle. The lifetime of each coil was determined based on breakdown during AC or pulse voltage testing. The results indicated a gradual decrease in IR, which remained relatively high even after 24,330 h of thermal aging at 175 °C. In contrast, tanδ and IC exhibited higher sensitivity to changes induced by thermal stress, with tanδ increasing due to the combined effects of polarization and conduction losses. Khowja et al. [19] measured the IR of twisted pairs aged at 250 °C, 270 °C, and 290 °C. IR gradually declined with aging time, and reductions of 82–90% were observed at 290 °C compared to unaged samples. Next, Khowja et al. [48] investigated the effects of thermal aging on the tanδ, IC, and PDIV of two different wire insulation materials. The results showed that during the aging process, the insulation layer experienced delamination, which caused an increase in tanδ and IC, while PDIV decreased. Additionally, a single-stress Arrhenius model was used to establish the lifetime model, and the thermal insulation rating of the two wires was estimated to be lower than that reported by the manufacturers. Gyftakis et al. [49] observed that thermal aging led to a homogenization of insulation resistance characteristics for thin-film insulation materials. No distinct aging curve for insulation resistance was evident over the aging period before breakdown. Table 1 summarizes the testing methods and characteristics of macroscopic aging indicators.

Table 1. Summary of testing methods and characteristics of macroscopic aging indicators.

Relevant Studies	Aging Indicators	Tests and Methods	Trends with Increasing Aging Time	Failure Criteria
[22,30,50]	RBV	Hi-pot tests	Decrease	Value > Criteria
[19,46,47]	IR	AC tip-up tests	Decrease	Value > Criteria
[44,47,48,51]	tanδ	AC tip-up tests	Increase	Value < Criteria
[39,45,46,48]	IC	AC tip-up tests	Decrease	Value > Criteria
[21,38,44]			Increase	Value < Criteria
[38,39,41–43,48]	PDIV	AC or pulse tests with PD sensors	Decrease	Value > Criteria
[42]	PDEV	AC or pulse tests with PD sensors	Decrease	Value > Criteria

2.4. Microscopic Aging Indicators

Unlike macroscopic indicators, microscopic aging indicators focus more on changes in the internal structure of materials, providing deeper insights into the aging mechanisms. Common microscopic indicators include microcrack density, void distribution, molecular weight changes in polymer chains, chemical functional group content, and the degree of carbonization. For example, scanning electron microscopy (SEM) observations reveal

that thermal aging leads to the formation of microcracks and voids on the surface of insulating materials, and these microstructural defects often serve as the initiation points for macro-level failure. Fourier-transform infrared spectroscopy (FTIR) and thermogravimetric analysis (TGA) are capable of revealing changes in chemical bonds and mass loss during the aging process. Additionally, the quantification of the degree of microscopic carbonization can reflect the progress of the thermal oxidation process, providing a reliable basis for model development.

Liao et al. [52] conducted a study on the changes in the microstructure, fiber structure, and ultrastructure of insulating paper during thermal aging. By comparing atomic force microscopy images of insulating paper samples, it was found that the atomic arrangement of cellulose in the initial insulating paper was dense and ordered. However, after accelerated thermal aging, the hexagonal structure of the glucose monomer was disrupted. Furthermore, scanning electron microscope images revealed that the cellulose cell walls gradually fractured during the aging process, and both the length and thickness of the cellulose fibers were reduced. X-ray diffraction analysis showed that the crystallinity and grain size of the insulating paper samples gradually decreased during aging, although the original cellulose crystal form and the coexistence of two-phase microstructures were still maintained. Mezgebo et al. [53] developed an algorithm to estimate the aging of insulating paper using subsurface structural images obtained via scanning-source optical coherence tomography (OCT). Figure 5 shows a comparison of OCT images of the samples before aging and after 152, 252, and 396 h of aging at 140 °C. The typical morphological changes of oil-impregnated paper due to thermal aging can be clearly observed, such as the appearance of cracks between the fibers and a reduction in fiber density. By performing texture analysis on the acquired images and extracting features, the aging degree of the insulating paper can be quantified.

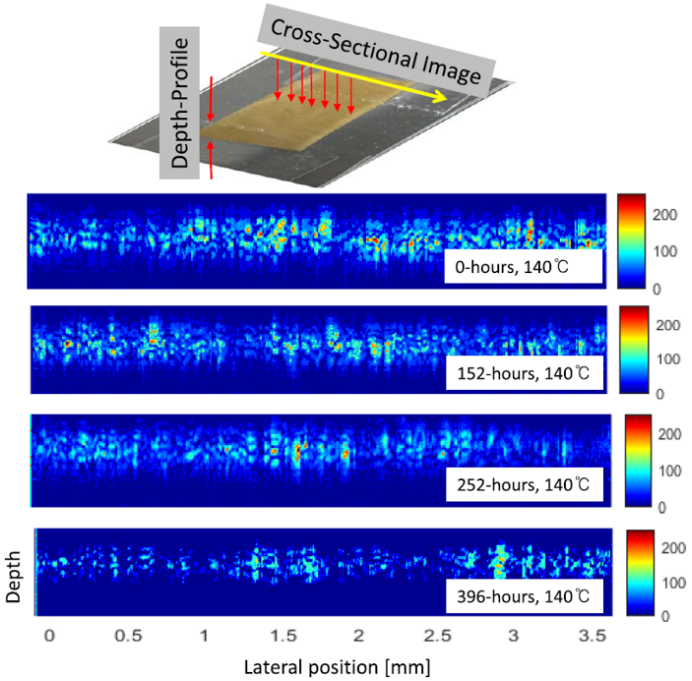

Figure 5. A comparison of the OCT images of the samples before aging and after 152, 252, and 396 h of aging at 140 °C [53].

Zhou et al. [54] conducted thermal aging tests on ethylene–propylene rubber cables used in electric locomotives and performed FTIR, SEM, and other tests on the samples. The results indicated that under prolonged thermal stress, the absorption peaks of the

original groups in the insulation layer underwent significant changes. Compared to the new samples, the aged samples showed irregular grooves on the surface, with white particles indicating different degrees of precipitation, leading to the formation of small pores. The white particles were caused by the migration, diffusion, and accumulation of additives within the sample, while the small pores resulted from gas adsorption or surface volatilization [55,56]. SEM images of the samples at different aging stages revealed that as aging progressed, the sample surface became rougher, the density of white particles increased, and the particle size grew from 1.4 μm in the unaged state to approximately 10 μm. Kong et al. [11] systematically studied the dielectric properties of epoxy resin at 180 °C over different aging periods and elucidated the mechanisms behind these changes from the perspective of microstructural alterations. As the thermal aging time increased, the cross-linking network of the epoxy resin was gradually destroyed, leading to an increase in the number of charge carriers, and a reduction in trap energy levels and densities. This enhanced dielectric polarization and charge injection, resulting in a significant decrease in the PDIV and BV. With increasing aging time, the appearance of the epoxy resin visibly changed, characterized by a gradual darkening of the color, as shown in Figure 6. After 1440 h of aging, the color changed from light yellow to dark brown and finally to black. Furthermore, when the aging time was less than 168 h, oxidation mainly occurred on the sample's surface, causing a color difference between the surface and the interior. After 168 h, the surface and interior colors of the epoxy resin became similar, indicating that thermal oxidative aging occurred uniformly throughout the sample. SEM images of the epoxy resin showed that as aging time extended, the surface transitioned from smooth to degraded damage, with incomplete pores and cracks beginning to appear, as shown in Figure 7. Additionally, slight warping around irregular voids became more noticeable. After 1440 h of aging, the damage to the epoxy resin intensified, with increased fragmentation, greater particle precipitation, and a larger number and area of cracks and voids. The infrared spectroscopy results in Figure 8 indicated that the intensity and wavenumber shifts of absorption peaks for different groups effectively reflected the extent of aging. The differential scanning calorimeter (DSC) curves of epoxy resin at various aging levels showed that the glass transition temperature (T_g) initially increased and then decreased with the extension of aging time, as shown in Figure 9. Hao et al. [57] analyzed the chemical formula of mica crystals using X-ray diffraction and explored the aging process of mica through diffraction patterns. Additionally, they conducted TGA and FTIR on the aging process of epoxy in stator insulation. The results indicated that the aging mechanism of epoxy in stator insulation involves side-chain oxidation and main-chain cleavage. Wu et al. [15] observed that as the aging degree of polyimide films increased, significant pores appeared on the surface, resulting in increased surface roughness. Yang et al. [16] used atomic force microscopy to observe that polyimide films gradually carbonized with aging, and the color gradually darkened. Cavallini et al. [39] provided microscopic images of samples under scanning electron microscopy before and after 300 h of aging, noting that although no obvious aging cracks were observed, some crystalline structures were detected. Zheng et al. [58] proposed a new method to evaluate the aging of oil–paper insulation using the fluorescence characteristics of suspended fibers in oil. They conducted accelerated thermal aging tests on oil–paper insulation at 120 °C and 130 °C, obtaining fibers with varying degrees of aging. Using a fluorescence characteristic testing platform, they measured the fluorescence emission spectra and excitation spectra of these fibers. The results showed that with increasing aging, the fluorescence intensity decreased, and the fluorescence peak gradually redshifted.

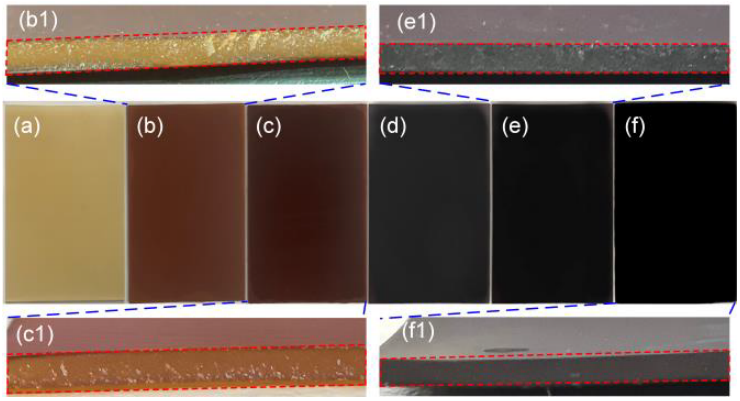

Figure 6. Changes in appearance after aging at (**a**) 0 h, (**b**) 72 h, (**c**) 168 h, (**d**) 336 h, (**e**) 672 h, and (**f**) 1440 h, and in cross-sections of the samples at (**b1**) 72 h, (**c1**) 168 h, (**e1**) 672 h, (**f1**) 1440 h [11].

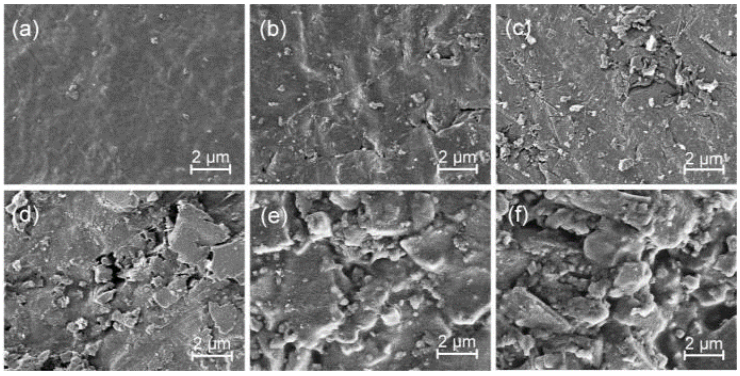

Figure 7. SEM images of the epoxy resin after aging at (**a**) 0 h, (**b**) 72 h, (**c**) 168 h, (**d**) 336 h, (**e**) 672 h, and (**f**) 1440 h [11].

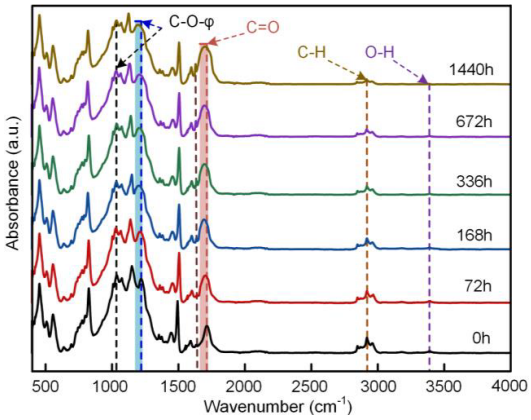

Figure 8. Infrared spectra of various samples under different aging conditions [11].

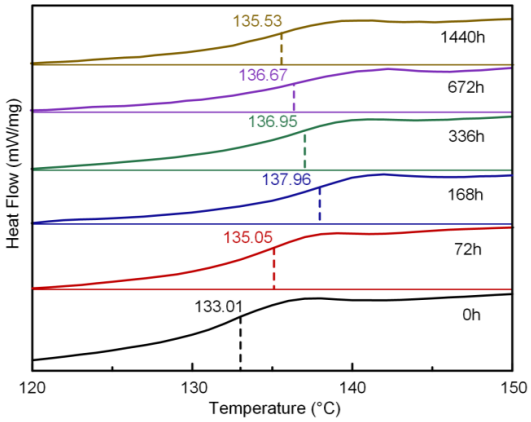

Figure 9. DSC curves of various samples under different aging conditions [11].

It is worth noting that while microscopic aging indicators are complex, they hold significant potential for application in predictive models, especially within data-driven approaches and multi-field collaborative analysis frameworks. The integration of these microscopic details can further enhance the accuracy and reliability of lifetime prediction. Table 2 provides a summary of the testing methods and characteristics of microscopic aging indicators.

Table 2. Summary of testing methods and characteristics of microscopic aging indicators.

Relevant Studies	Aging Indicators	Tests and Methods	Features with Increasing Aging Time
[11,16]	Color	Image	Gradual darkening
[16,52]	Atomic arrangement of cellulose	Atomic force microscope	Bond breakage between atoms; sparse arrangement; enlargement of voids
[11,15,39,52,54]	Cracks on fiber surface; diameter of white particles	SEM	Reduction in length and roughness; increase in particle size
[11,54,57]	Absorbance	FTIR	Decrease
[11,57]	T_g	TGA	Initial increase followed by decrease
[52,57]	Grain size	X-ray diffraction	Decrease
[53]	Haralick texture features	OCT	Decrease
[58]	Fluorescence intensity	Fluorescence characteristic test platform	Decrease

3. Physics-of-Failure-Based Insulation Lifetime Modeling

PoF is a fundamental approach to reliability analysis, focusing on understanding and modeling the mechanisms that drive the failure of EIS. Unlike data-driven models that rely on statistical correlations, PoF models are based on the physical and chemical processes underlying degradation. This approach provides a deeper understanding of the behavior of EIS under thermal stress, enabling more accurate and generalizable lifetime prediction. This section focuses on the application of PoF methods for modeling the lifetime of motor insulation under thermal aging, providing a detailed introduction to the modeling framework and case studies.

3.1. Theoretical Foundations of PoF

One of the main challenges in applying PoF methods is determining the insulation stresses and selecting the appropriate lifetime model. In practical applications, aging stresses often act simultaneously on the EIS, and thus, a multi-stress lifetime model is required to achieve representative lifetime predictions. Although multi-stress models provide high accuracy, their complexity arises from the inability to apply the superposition principle, which makes it difficult to distinguish and quantify the contributions of two or more aging factors acting concurrently (i.e., coupled or combined aging effects) [59]. To address these challenges, another approach is to identify the primary aging mechanisms, establish a single-stress model, and then extend or integrate it into a comprehensive model [5]. The hypothesis of a dominant aging factor is widely adopted in the literature [2,60,61] and standards [1]. In a typical operational cycle, most insulation systems are primarily affected by a single dominant stress. Their lifetime is mainly determined by this dominant stress, and the influence of other stresses (i.e., secondary aging factors) is considered negligible.

Therefore, using a single-stress lifetime model for insulation lifetime prediction is a practical and effective method. This review particularly focuses on thermal stress as the primary aging factor.

3.2. Lifetime Modeling Process Under Thermal Stress

The oxidation process causing insulation aging under thermal stress is a first-order chemical reaction, and its reaction rate can be described using the Arrhenius law. The lifetime model based on the Arrhenius equation, proposed by Dakin, has been widely used to describe thermal aging lifetime [2,3,20,29,62–67], as follows:

$$L(T) = a \exp(b/T), \tag{1}$$

where $L(T)$ is the thermal life of the insulation at temperature T, and a and b are parameters that depend on the properties of the material. After collecting sufficient failure data from accelerated constant thermal aging tests, the parameters a and b can be solved to obtain the explicit expression for the insulation's lifetime, which can be directly used to predict the expected thermal lifetime of electrical machine insulation at a specific temperature. However, when the motor operates under a non-stationary load condition, the internal temperature is usually variable. Using only a single temperature value from the variable temperature profile for lifetime prediction leads to inaccurate results. For instance, using the maximum temperature for lifetime prediction yields overly conservative results. On the other hand, using the minimum or average temperature may lead to estimates that carry potential risks. To address lifetime prediction under variable temperatures, the cumulative damage law was combined with the Arrhenius equation in the literature [68], providing more accurate results. As shown in Figure 10, a time-varying temperature curve with a cycle period of Δt_{cycle} is considered. For each infinitesimal time interval dt in the temperature profile, the temperature can be treated as constant, $T_i(t)$, and thus Equation (1) can be directly applied. The lifetime loss fraction dLF for the time interval is then calculated as follows:

$$dLF = \frac{dt}{L[T_i(t)]}. \tag{2}$$

By integrating the entire temperature curve, the lifetime loss LF under the temperature profile Δt_{cycle} can be obtained:

$$LF = \int_0^{\Delta t_{cycle}} dLF = \int_0^{\Delta t_{cycle}} \frac{dt}{L[T_i(t)]}. \tag{3}$$

Considering the number of thermal stress cycles experienced by the motor insulation, the total lifetime L_{tot} is calculated as:

$$L_{tot} = \frac{1}{LF} \cdot \Delta t_{cycle}. \tag{4}$$

Equations (1) and (4) can be used to accurately estimate the thermal lifetime under both constant and variable temperature profiles. Additionally, for failure data obtained from accelerated thermal cycling tests, the lifetime model must be appropriately adjusted to account for the additional lifetime loss of the motor under variable temperature aging [29].

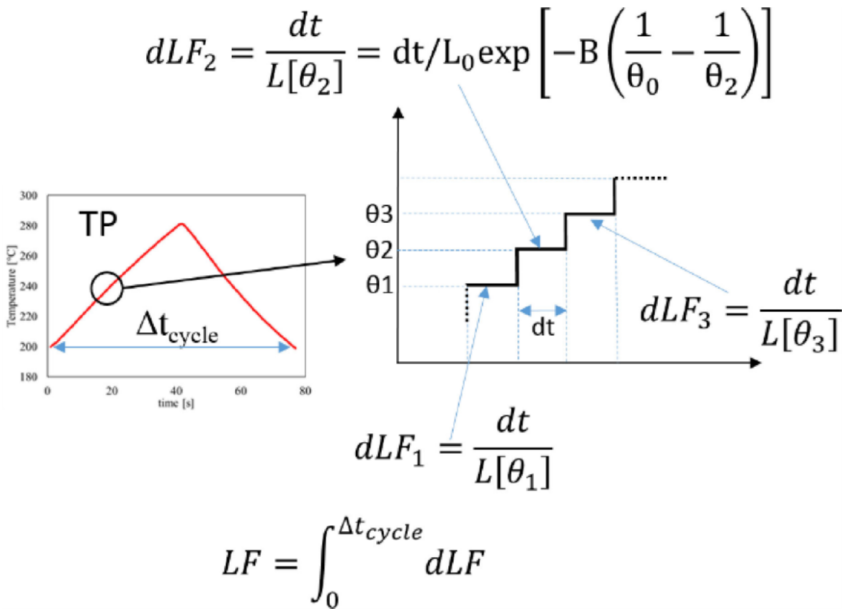

Figure 10. The computation of the loss of life under a time-varying temperature curve [3].

3.3. Application of the PoF Model in Insulation Lifetime Prediction

To illustrate the application of the PoF model, the lifetime prediction of electrical machine insulation under thermal aging is considered. Giangrande et al. [2] conducted accelerated aging tests on the motorettes at temperatures of 230 °C, 250 °C, and 270 °C, with aging cycles of 384 h, 96 h, and 24 h, respectively. Five motorettes were aged at each determined temperature, for a total of 30 coils. After each aging cycle, dielectric breakdown tests were performed on the samples, with the BV used as the lifetime end criterion. The applied voltage should be less than the PDIV value measured in the tests to satisfy the assumption of no PD in low-voltage motors. It is important to note that the choice of lifetime criterion does not affect the validity of the modeling analysis. The purpose of developing a lifetime prediction model is to use failure times collected from accelerated thermal aging tests to infer the failure time distribution under normal operating conditions, considering different percentiles [69]. Since there are multiple failure time data points under the same thermal stress level, the Weibull distribution is commonly and widely used to handle failure intervals related to insulation breakdown [70,71]. The cumulative distribution function (CDF) of the Weibull distribution, $F(t)$, can be expressed as:

$$F(t) = 1 - \exp\left[-\left(\frac{t}{\alpha}\right)^{\beta}\right], \tag{5}$$

where α is the scale parameter, representing the time required for 63.2% of the samples to reach the end of life, and β is the shape parameter, indicating the variability of the data. These parameters can be solved using a linear regression approach, with the detailed solution process found in [2]. Weibull probability plots with 95% confidence intervals for failure times at the three different temperatures are shown in Figure 11. The result indicates that an increase in temperature significantly reduces the thermal lifetime of the insulation, as reflected by the decrease in the shape parameter. Due to the material's glass transition effect and enamel shedding, the failure data at 270 °C exhibited considerable variation, leading to an increase in the shape parameter. To derive the lifetime under standard operating conditions, the thermal endurance curve of the samples must be extrapolated. Weibull distribution with different percentiles was used to determine the Arrhenius curve. For instance, at the 10th percentile (B10) and the 50th percentile (B50), the resulting Arrhenius

curves are shown in Figure 12. It is important to note that Figure 12 shows only the lifetime curves at two percentiles. Any other percentiles can be used depending on the required reliability level. The corresponding lifetime model in [2] is:

$$\begin{cases} L_{B10}(T) = 1.9 \times 10^{-12} \exp\left(\dfrac{16028}{T}\right) \\ L_{B50}(T) = 3.5 \times 10^{-11} \exp\left(\dfrac{17793}{T}\right) \end{cases}. \quad (6)$$

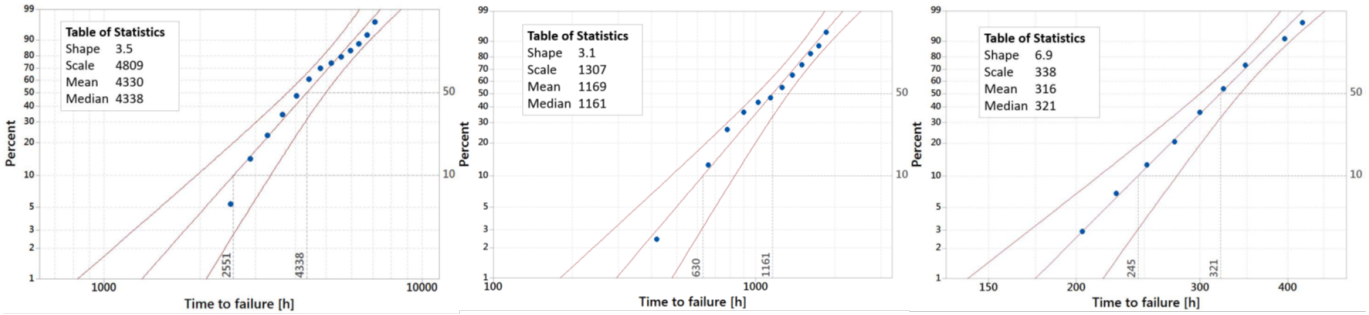

(a) (b) (c)

Figure 11. Weibull probability plot for the time-to-failures at (a) 230 °C, (b) 250 °C, and (c) 270 °C [2].

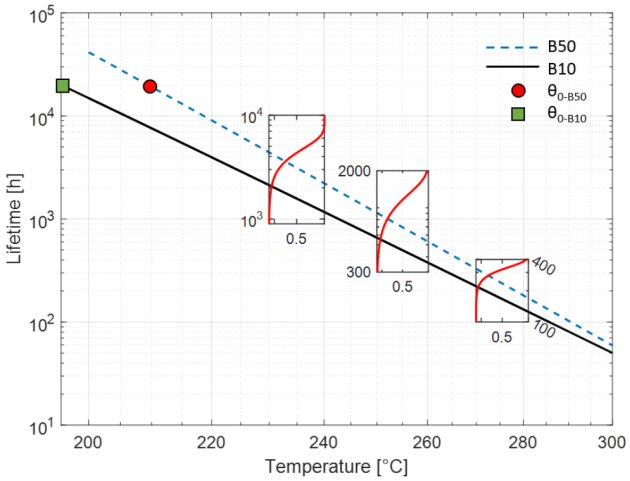

Figure 12. Experimental Arrhenius curves at B10 and B50 of the Weibull CDFs and thermal classes with 20,000 h lifetime at B10 and B50 [2].

Based on the established lifetime model, the thermal lifetime of EMs under both continuous operation (i.e., constant temperature) and variable duty cycle operation (i.e., varying temperature) can be predicted.

To study the effect of variable temperature aging on insulation thermal lifetime, Zhou et al. [29] used the PoF model to examine the additional lifetime loss induced by variable temperature aging and demonstrated these differences through the equivalent temperature method. The derivation process of the equivalent temperature is illustrated in Figure 13. The initial Arrhenius model was derived from lifetime data under three constant thermal stress levels. For example, the variable temperature profile TP1 with a range of 220–260 °C and a period of 80 s was analyzed to assess the additional lifetime loss. The lifetime L_E obtained from the experiment at TP1 was 204 h, whereas using the temperature curve of TP1 in the variable temperature Arrhenius model, the lifetime L_A calculated was 403 h. This result indicates that the lifetime termination due to temperature variation is about 50% lower than the value derived from the previous lifetime model. By substituting L_E and L_A into the original Arrhenius model, the equivalent temperatures

θ_E and θ_A were calculated as 260 °C and 242 °C, respectively. The temperature variation induced an additional thermal aging effect of 18 °C. Therefore, for lifetime prediction under variable temperature conditions, the traditional PoF-based models that assume a single aging stress will exhibit prediction bias due to the introduction of additional thermo-mechanical stresses. More experiments are needed to improve the research results, and lifetime models more generally applicable to variable temperature applications should be developed.

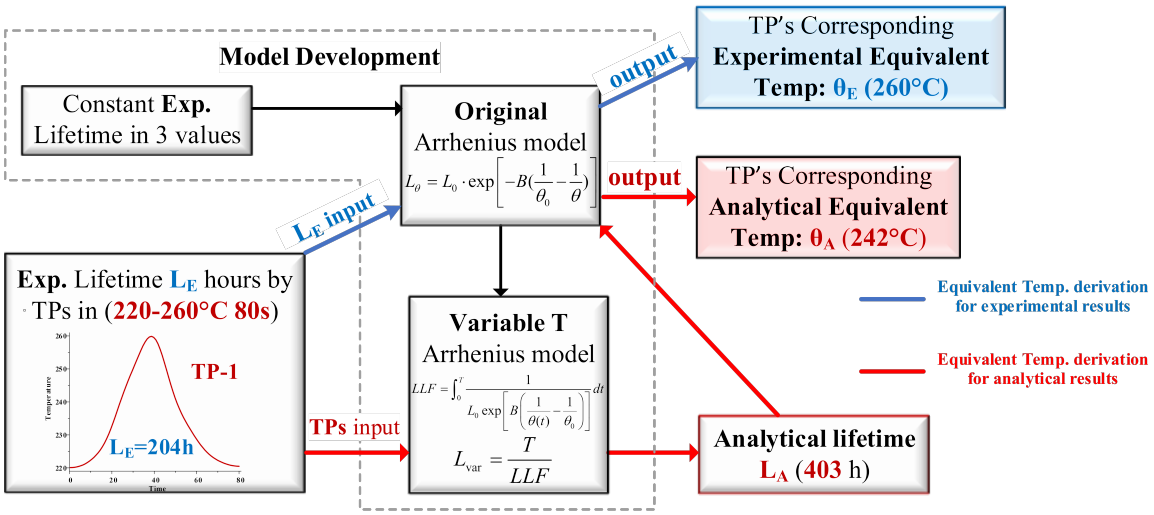

Figure 13. Relationship between experimental and analytical results (in B10) [29].

3.4. Advantages and Limitations

PoF-based insulation lifetime modeling offers several distinct advantages. By establishing the model on the fundamental aging mechanisms, it provides a physically interpretable framework that allows researchers to identify and target key factors influencing insulation performance. This interpretability not only aids in a deeper understanding of failure modes but also contributes to the development of tailored material improvements. Moreover, the POF model is highly adaptable and can be applied to various stress conditions, including thermal, electrical, and mechanical factors, making it a universal tool for various insulation systems. Additionally, when supported by reliable experimental data, these models exhibit strong predictive accuracy, especially in cases where a single stress dominates.

Despite these advantages, PoF models face significant limitations. One major challenge is accurately modeling complex multi-stress scenarios, where interactions between stresses may complicate the identification of failure mechanisms and the selection of appropriate lifetime models. In determining model parameters, a large amount of experimental work is often required under controlled conditions, which can be resource-intensive. Furthermore, PoF-based lifetime models are primarily used during the early design stages of motors, providing valuable insights for material selection and structural optimization. However, their application to motors in operation remains limited. In real-world scenarios, variability in operating conditions, the impact of unexpected stress factors, and potential long-term cumulative effects present challenges that current models cannot fully address. These limitations highlight the need for further improvements and innovations in PoF-based modeling to enhance its applicability and accuracy in practical insulation reliability assessments.

4. Data-Driven-Based Insulation Lifetime Modeling

With the rapid development of AI technologies, data-driven lifetime modeling methods have demonstrated broad application prospects in the field of insulation aging prediction. Unlike PoF-based models, these methods capture complex nonlinear relationships through the deep learning and pattern mining of experimental data, achieving higher prediction accuracy. Particularly in accelerated thermal aging experiments, data-driven models are constructed by collecting key performance parameters (such as BV, IR, and IC), offering a new solution for predicting the lifetime of electrical machine insulation. This chapter reviews the data-driven modeling approaches and their applications proposed in the existing literature, with a focus on the modeling process, algorithm selection, practical applications, and a discussion of their advantages and limitations.

4.1. Data-Driven Modeling Process

Data-driven insulation lifetime modeling relies on high-quality experimental data. The modeling process primarily consists of four stages: data collection and preprocessing, feature selection and dimensionality reduction, model selection and training, and model validation and prediction. The collection of key performance parameters from accelerated aging experiments under various temperature stresses forms the foundation of data-driven modeling. Additionally, data preprocessing is a crucial step in the modeling process, which involves the removal of outliers, data normalization, and the extraction of key features to ensure the quality and relevance of the input data. Feature selection and dimensionality reduction play a key role in building an efficient model. Through correlation analysis and other methods, features closely related to lifetime are extracted as input variables for the model. Another approach involves using principal component analysis (PCA) to reduce the dimensionality of high-dimensional data, simplifying model complexity and improving computational efficiency. Model selection and training are the core aspects of the data-driven modeling process. Based on the characteristics of the experimental data, common AI algorithms such as neural networks (NNs), support vector machines (SVMs), and random forests (RFs) can be selected [72,73]. These algorithms learn and train on experimental data, gradually optimizing model parameters to capture underlying patterns within the data. Finally, model validation and prediction are conducted through cross-validation and independent test sets to evaluate the model's performance. This stage not only assesses the predictive accuracy of the model but also analyzes its sensitivity to lifetime variations under different temperature stresses. The validation results will directly influence the model's reliability in practical applications.

4.2. Application of the AI Algorithms in Insulation Lifetime Prediction

AI algorithms are widely applied in lifetime prediction tasks due to their powerful nonlinear fitting capabilities. A typical NN architecture is shown in Figure 14. It generally consists of 3 to 4 layers, including an input layer, 1 to 2 hidden layers, and an output layer. Each node in the input layer corresponds to an input variable, and these nodes pass the raw data to the next layer. The hidden layers perform feature extraction and transformation on the input data, calculating weights using an activation function to capture complex patterns and relationships in the input data. In the output layer, the final prediction or decision output is produced, with the predicted values expressed with the corresponding estimation errors [74].

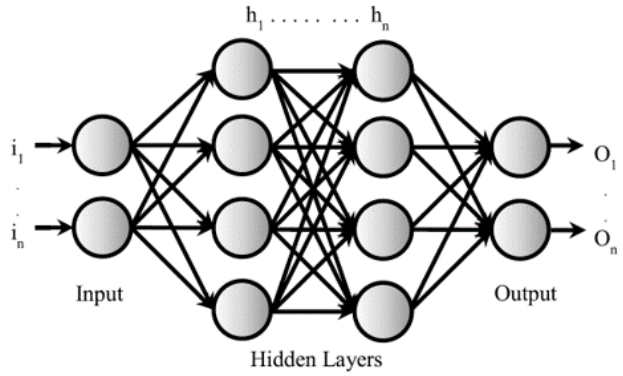

Figure 14. The general architecture of the NN [75].

Mokhnache et al. focused on utilizing artificial neural network (ANN) technology to predict the thermal aging characteristics and lifetime of transformer oil and other high-voltage insulating materials. These studies collected electrical and physical performance data of various insulating materials, including transformer oil, at different temperatures and times through experiments [76–81]. In [76], a radial basis function Gaussian network (RBFG) was used, trained using a random optimization method (ROM) and two learning techniques (i.e., data-adaptive learning and batch learning). The designed network provided relative errors of 5% and 3% under the two learning techniques, respectively. The predicted results were comparable to long-term test results in the laboratory, providing strong data support for the thermal aging prediction of transformer oil. In [77], various ANN algorithms were applied to diagnose and predict the thermal aging of transformer oil. The diagnostic network errors varied with the algorithms used, but the results were good and contributed to reducing aging experiment time and improving diagnostic quality. In [78], the performance of two training algorithms, Levenberg–Marquardt (LM) and back propagation (BP), were compared for testing the RBFN. The results indicated that the BP algorithm provided better predictions than the LM algorithm. Additionally, in [79], the tensile strength of insulating paper and BV of insulating oil were measured at different temperatures. Using partial aging data, an RBFG network was trained to predict the trend of insulation performance changes over a longer time range. Further extending the research, in [80,81], the trained models were applied to predict the BV of high-voltage liquids, solids, and gaps. The results showed excellent consistency with experimental results and were able to accurately predict nonlinear curves.

Certain studies [82,83] employed ANNs to predict the performance changes of XLPE materials during thermal aging, aiming to reduce the time and cost associated with traditional experimental methods. Initially, the researchers systematically studied the thermal aging effects of commercial XLPE materials at different temperatures using experimental methods, measuring key mechanical properties such as elongation at break and tensile strength. Subsequently, they constructed a supervised neural network based on the RBFG model, trained using BP and ROM. Additionally, Kohonen maps were utilized as an unsupervised NN approach. By comparing experimental data with ANN-predicted results, the study confirmed the effectiveness of ANNs in modeling XLPE material performance degradation. ROM, in particular, demonstrated superior predictive performance due to its independence in weight adjustment and generalization capability. Furthermore, ref. [82] extended the study to predict the lifetime of XLPE materials, comparing the results with the traditional least-squares method (LSM), which showed excellent consistency. The researchers also explored the impact of training time on network learning quality, revealing an optimal training duration for achieving better learning outcomes [83]. This research not only provided deep insights into the aging behavior of XLPE cable insulation materials but

also proposed a novel technological pathway for the rapid prediction of material performance. Ref. [84] introduced a BPNN-based method for predicting the dielectric loss factor, aiming to improve the application level of online monitoring and diagnosis for capacitive equipment. The study employed a carefully designed three-layer BPNN model, accounting for environmental factors such as temperature and humidity affecting the dielectric loss values. By optimizing the configurations of the input and output layers and experimentally selecting the number of neurons in the hidden layer, the model achieved high-precision predictions of the dielectric loss factor. Simulations conducted using MATLAB software validated the effectiveness of the method, with prediction errors meeting engineering requirements. This approach provides scientific support for preventing high-voltage insulation accidents. Ref. [85] explored the use of NN to predict the IR changes in electrical networks with isolated neutral points. After initial attempts with multilayer perceptron NN failed to meet expectations, the researchers adopted a long short-term memory (LSTM) recurrent neural network (RNN). LSTM networks were selected for their ability to capture long-term dependencies in time-series data. By collecting data on IR, temperature, and humidity, the researchers trained the LSTM model and successfully predicted IR changes, keeping prediction errors within a small range. This study demonstrated the potential and effectiveness of LSTM networks in handling highly noisy time-series data and predicting EIS performance. Ref. [75] proposed a novel NN approach trained with Bayesian regularized back propagation (BRP) algorithm, illustrated in Figure 15, to predict the thermal lifetime of motor insulation materials. This method significantly improved testing efficiency by reducing the required time for ADTs. At aging temperatures of 250 °C, 270 °C, and 290 °C, the BRP-based NN was used to predict the IR of twisted pairs and compared with traditional lifetime evaluation methods. The results showed that the BRP-based NN predictions aligned well with experimental outcomes, with a relative error in temperature index of only 0.125% compared to traditional methods. By using the BRP for predicting the thermal lifetime of insulation materials, 57% of the testing time was saved, equivalent to a reduction of 1680 h, offering an efficient and accurate new tool for assessing the thermal lifetime of motor insulation materials.

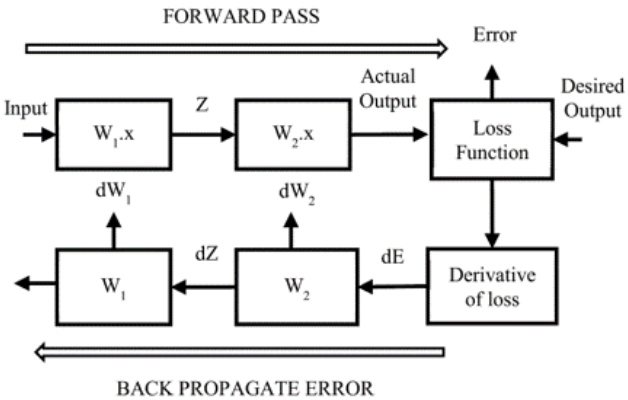

Figure 15. NN architecture of BRP algorithm in [75].

Furthermore, CF has been recognized as an effective data-driven approach for rapidly predicting insulation lifetime [21]. In [86], the combined application of NNs and CF methods was explored to evaluate the lifetime of enamel wire IR under thermal aging conditions. The study employed a BPNN alongside three different CF models—exponential, logarithmic, and power series (as shown in Equations (7)–(9)). These methods were used to estimate the trend of IR and the mean time-to-failure (MTTF) of the samples. Through thermal aging tests conducted at a high temperature of 290 °C, the researchers observed that the BPNN outperformed traditional CF methods in predicting IR trends and MTTF.

Specifically, the BPNN demonstrated the highest prediction accuracy, with a relative error of only 3.29% compared to conventional lifetime evaluation methods. In contrast, all three CF models exhibited errors exceeding 10%. The corresponding prediction results, illustrated in Figure 16, highlight the superior accuracy and reliability of neural networks in forecasting insulation performance. This study underscores the potential of NNs, combined with traditional CF techniques, to enhance the precision and efficiency of insulation lifetime predictions under thermal aging conditions.

$$y(t) = A\exp(Bt), \tag{7}$$

$$y(t) = m \cdot \ln(t) + c, \tag{8}$$

$$y(t) = Pt^d, \tag{9}$$

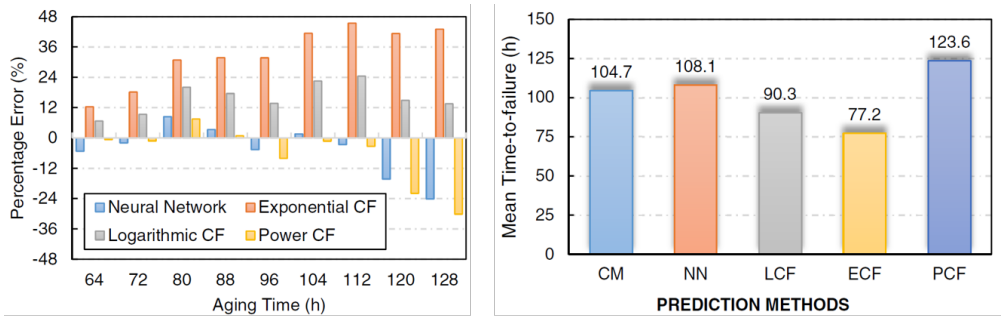

Figure 16. (**a**) Percentage error comparison of specimen S9, (**b**) Comparison of mean time-to-failure in [86].

Building on previous research, [19] utilized three CF models—exponential, logarithmic, and power law—to predict IR and compare their performance with the BRP-based NN and traditional lifetime estimation methods. The study focused on samples subjected to thermal stress at 250 °C, 270 °C, and 290 °C. It predicted IR trends and determined time-to-failure based on end-of-life criteria. For each thermal stress level, the MTTF was calculated using log-normal probability curves, and a thermal lifetime model was developed based on the MTTF values. The results showed that while the logarithmic CF model outperformed other CF approaches in prediction accuracy, it was still less precise than the BRP-based NN model. The error rates for thermal index comparisons with standard methods were 0.95% for the logarithmic CF model and 0.17% for the BRP-based NN. In addition to accuracy, the study highlighted time savings: the logarithmic CF model reduced testing time by 83 days, while the BRP-based NN method saved 71 days compared to standard lifetime evaluation procedures. These findings underscore the trade-offs between accuracy and efficiency in employing NNs and CF methods. Both approaches demonstrated their capability to significantly reduce testing duration while maintaining satisfactory prediction accuracy, making them valuable alternatives for insulation material lifetime assessments.

4.3. Advantages and Limitations

Data-driven lifetime modeling methods offer advantages such as efficient modeling capabilities, flexible adaptability, and significant savings in experimental resources. Through AI algorithms, these methods can capture complex nonlinear relationships in accelerated aging data and adapt to various insulation materials and experimental conditions. However, several limitations are associated with these approaches, including a reliance on high-quality data, a lack of model transparency, and limited generalization capability under untested experimental conditions.

5. Stochastic Process-Based Insulation Lifetime Modeling

Stochastic processes are mathematical tools used to describe the uncertainty in the evolution of systems over time, with significant applications in lifetime prediction. For the thermal aging process of EIS, where degradation exhibits randomness and irreversibility, stochastic process-based methods provide a more realistic description than deterministic models. This section explores the theoretical foundation, primary methods, and applications of stochastic process modeling in insulation lifetime prediction, along with an analysis of its advantages and limitations.

5.1. Theoretical Foundation of Stochastic Processes

The degradation of product performance metrics is influenced by numerous known and unknown external factors, leading to inherent randomness in the degradation process. Consequently, recent years have seen a shift in research focus toward using stochastic process models to describe performance degradation, yielding significant results. Among these models, the Wiener process [17,50,51,87–89] and the Gamma process [90,91] are the most widely applied.

Let $Y(t)$ represent the degradation at time t. For a Wiener process, the degradation model can be expressed as:

$$Y(t) = \mu t + \sigma B(t) + y(0), \tag{10}$$

where μ is the drift parameter of the Wiener process, σ is the diffusion parameter, $B(\cdot)$ is the standard Brownian motion, and $y(0)$ is the initial amount of degradation.

If the performance indicator of a product follows a Wiener degradation process $Y(t)$, and D denotes the failure threshold of the performance indicator, the lifetime L is defined as the first passage time (FPT) of $Y(t)$ crossing D:

$$L = \inf\{t | Y(t) \geq D\}. \tag{11}$$

Based on the properties of the Wiener process, the lifetime L of motor insulation follows an inverse Gaussian distribution. Its probability density function (PDF) $f_L(t)$ and cumulative distribution function $F_L(t)$ can be expressed as:

$$f_L(t) = \frac{D}{\sqrt{2\pi\sigma^2 t^3}} \exp\left[-\frac{(D-\mu t)^2}{2\sigma^2 t}\right], \tag{12}$$

$$F_L(t) = \Pr(L \leq t) = \Phi\left(\frac{\mu t - D}{\sigma\sqrt{t}}\right) + \exp\left(\frac{2\mu D}{\sigma^2}\right)\Phi\left(-\frac{\mu t + D}{\sigma\sqrt{t}}\right), \tag{13}$$

where $\Phi(\cdot)$ is the cumulative distribution function of the standard normal distribution. The reliability function $R_L(t)$ can be expressed as:

$$R_L(t) = 1 - F_L(t) = \Phi\left(\frac{D - \mu t}{\sigma\sqrt{t}}\right) - \exp\left(\frac{2\mu D}{\sigma^2}\right)\Phi\left(-\frac{\mu t + D}{\sigma\sqrt{t}}\right), \tag{14}$$

For systems where degradation is better characterized by a Gamma process, the degradation model is expressed as:

$$Y'(t) \sim Ga(\alpha t, \beta). \tag{15}$$

where α is the shape parameter and β is the scale parameter. The reliability function $R'_L(t)$ of the product can then be derived as [92]:

$$R'_L(t) = 1 - \frac{\Gamma(\alpha t, D\beta)}{\Gamma(\alpha t)}. \tag{16}$$

From this, the reliable lifetime L_R can be calculated, providing a quantitative measure of product lifetime.

5.2. Performance Degradation Modeling Based on Stochastic Processes

When the degradation process of a product exhibits monotonic behavior, the Gamma process is a suitable tool for modeling the degradation trajectory. The Gamma process was first introduced by Mohamed [93] to describe system degradation. Later, Singpurwalla demonstrated the relationship between the Gamma process and the compound Poisson process, where the Gamma process can be seen as the limiting form of a compound Poisson process when the arrival rate approaches infinity and the jump size approaches zero [90,94]. Park et al. [95] applied the Gamma process to model metal crack degradation data and estimated the mean failure time. Lawless et al. [96] derived the failure lifetime distribution function for products with varying individual differences based on the Gamma process. Wang et al. [92] demonstrated that under accelerated stress conditions, the shape parameter of the Gamma process is related to the applied stress, while the scale parameter remains unchanged. By considering individual differences, prior distributions for degradation parameters were obtained using both conjugate and non-conjugate priors, and Bayesian methods were used to update degradation data for individual products. The Gamma process has also been applied in various fields such as concrete drainage systems [97], batteries [98], photovoltaic modules [99], and LEDs [100]. However, the complexity of the mathematical expressions for the Gamma distribution poses challenges for analytically updating degradation parameters with real-time monitoring data, limiting its application in remaining useful lifetime (RUL) prediction.

In contrast to the Gamma process, which is suitable only for monotonic degradation, the Wiener process can model both monotonic and non-monotonic degradation. Its well-established mathematical properties, including analytical solutions and statistical characteristics, make it an attractive choice for degradation modeling. The Wiener process was first used for degradation modeling by Bhattacharyya and Fries [101], who studied the physical interpretation of inverse Gaussian lifetime distributions. They assumed that cumulative fatigue damage follows a linear Wiener process and derived that the product's lifetime follows an inverse Gaussian distribution. One major advantage of the linear Wiener process is its ability to analytically describe the lifetime of degraded products, making it widely popular for degradation modeling. Building on the linear Wiener process, Doksum and Hbyland [102] developed variable accelerated lifetime testing models for degraded products. Guerin et al. [103] applied the linear Wiener process to model the wear of disc brakes, while Caglar et al. [104] used it to analyze vibration signals in accelerated aging tests of EMs. To address non-linear degradation processes, Whitmore et al. [105] and Wang et al. [106] proposed replacing the time parameter t with a time-scale transformation function $\Lambda(t)$. Additionally, Si et al. [107] assumed that the drift and scale parameters are time-dependent, thereby developing non-linear Wiener processes. By combining linear and non-linear Wiener processes, Wang et al. [108] proposed a unified degradation modeling framework for systems with both linear and non-linear degradation components. Zhang et al. [109] further explored non-linear Wiener processes where the drift and diffusion parameters depend on product lifetime and degradation state. Numerous researchers have introduced additional influencing factors into Wiener process models. For example, Whitmore [105] incorporated measurement errors into the Wiener process; Ye et al. [87] accounted for time-correlated error terms; Liao and Tian [110] and Liu et al. [111] assumed that the drift parameter is a function of covariates such as temperature or pressure; Ye et al. [112] extended this approach by considering both drift and diffusion parameters as functions of covariates; and Si et al. [107] and Peng and Tseng [113] modeled the diffusion

parameter as following a specific distribution to account for random effects. Through these advancements, the Wiener process has become a versatile and robust tool for modeling both linear and non-linear degradation, enabling comprehensive reliability analysis and lifetime prediction in various applications.

However, most degradation models based on stochastic processes assume a constant average degradation rate throughout the product's entire lifecycle. In practical applications, long-life and high-reliability products exhibit different statistical characteristics at various stages of degradation due to cumulative damage. Their degradation process often follows a multi-stage pattern, such as steady degradation, rapid degradation, and eventual failure [114]. Son et al. [115] described three stages of equipment operation: normal operation, soft failure, and hard failure. Gebraeel [116] conducted degradation tests on bearings, collecting vibration signals indicative of degradation levels, and observed a two-stage degradation process. To address this issue, researchers have recently started to analyze degradation processes by dividing them into two or more stages, proposing stochastic process models based on change points. Ng et al. [117] introduced a two-stage stochastic degradation model with independent increments based on a single change point, estimating model parameters using the expectation–maximization (EM) algorithm. Yan et al. [118] applied a two-stage Wiener process model for the reliability validation of hydraulic couplings, identifying change points based on the Schwarz information criterion (SIC). Chen et al. [119] improved a two-stage linear–logarithmic model to describe the phased degradation process of rolling bearings, updating model parameters using Bayesian methods for lifetime estimation. Wang et al. [120] divided the degradation process of liquid crystal displays into two stages, establishing Gamma and Wiener process models with change points, significantly improving the accuracy of reliability analysis. Ke et al. [121] developed a segmented degradation model based on the Wiener process to predict degradation paths. In the first stage, degradation progressed steadily and slowly; the likelihood function was derived using Bayes' theorem and the Markov property of Brownian motion, and parameters were estimated using the maximum likelihood method. In the second stage, Kalman filtering (KF) was applied to predict and correct current state values, with parameters estimated using the EM algorithm. Zhang et al. [122] derived a lifetime distribution under the first-passage-time framework within a two-stage Wiener process degradation model. This model's advantage lies in its ability to consider and quantify the uncertainty of degradation at the change point, with potential extensions to more general multi-stage degradation models.

5.3. Application of Wiener Process Model in Insulation Lifetime Prediction

Although degradation models based on the Wiener process have been widely applied in the degradation analysis and lifetime prediction of metal fatigue cracks [123], gyroscopes [124], and bearings [125], their application in predicting the lifetime of motor insulation under thermal stress remains limited.

Wang et al. [51] conducted an in-depth temperature field analysis and lifetime prediction study for the insulation system of a brushless DC motor. They first used Ansys Fluent software and computational fluid dynamics (CFD) methods to construct a three-dimensional temperature field model of the motor, analyzing the steady-state temperature distribution of the motor in air. The stator insulation was identified as the most affected component of the motor insulation system, with a maximum temperature of 381.1 K. Further, constant thermal stress ADTs were conducted on the insulation material, and its degradation was assessed using the insulation performance parameter (dielectric loss tangent, tanδ). Based on this, a failure threshold for performance degradation was established. Finally, a lifetime prediction model for the motor insulation was developed using the

Wiener process and Arrhenius model. The average lifetime of the motor insulation system under normal operating temperature was calculated to be approximately 23.41 years. Chen et al. [89] explored the lifetime prediction of permanent magnet synchronous motors (PMSMs) in a direct-drive selective compliance assembly robot arm (SCARA), with particular attention to the impact of thermal aging on the motor insulation. By constructing the kinematic and dynamic models of SCARA, they calculated the torque curve required by the motor to perform specific tasks. Combining accelerated thermal aging tests with the Wiener process, they developed a model for motor insulation degradation and derived the motor's reliability function. Through CFD simulation, they analyzed the temperature field distribution of the motor, using the highest temperature as the reference temperature for reliability evaluation. The results indicated that, in typical point-to-point tasks of SCARA as shown in Figure 17, the PMSM could run continuously for 102,623 h while meeting the 99% reliability requirement. This research not only provides deep insight into the long-term performance of motors but also offers crucial references for improving the overall reliability of robotic arms, thus supporting industrial automation production.

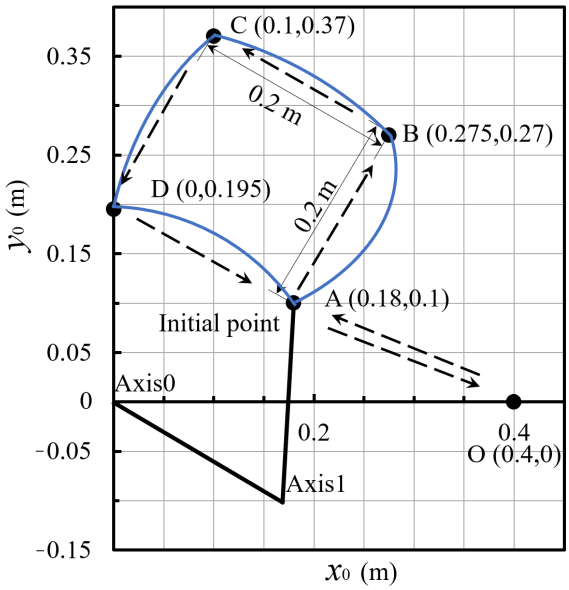

Figure 17. The typical point-to-point motion task diagram of direct-drive SCARA [89].

Wang et al. [17] proposed a new RUL prediction method for insulation materials exhibiting a two-stage degradation trend during accelerated thermal aging. This method can also be extended to other high-reliability products with two-stage degradation characteristics, as shown in Figure 18. In the offline phase, the change points in the two-stage accelerated degradation data were estimated using SIC and residual sum of squares minimum criterion (RSSMC). A statistical method was used to derive the distribution of these change points. Based on the estimated change points, a two-stage accelerated degradation model based on the Wiener process was established. After determining the unknown parameters, the model parameters related to the Wiener process and the change point distribution were extrapolated to any possible working stress level for overall lifetime prediction. In the online phase, the change points of field degradation data were detected in real-time by combining cumulative sum control chart (CUSUM) with the change point PDF of the working stress level. The accelerated aging data from two phases were transformed to the working stress level as prior information using acceleration factors. Bayesian methods were employed to update model parameters, yielding the estimated RUL and its corresponding PDF. Aging tests were conducted on typical insulation materials, poly-

imide film, at 290 °C, 300 °C, and 310 °C, collecting the maximum discharge amount at 300 h for each temperature as accelerated aging data. Based on the identified threshold, a reliability function for polyimide film was obtained, and the lifetime prediction results were validated at 270 °C. The experimental results showed that, compared with the single-stage Wiener process model that does not consider change points, the proposed two-stage model significantly improved prediction accuracy, especially after the insulation material entered the rapid degradation phase, where the prediction error rapidly decreased. This new method provides higher accuracy and lower uncertainty in predicting RUL, which is of great significance for health management and maintenance strategy formulation of high-reliability products. This research not only enriches the theory of lifetime prediction based on degradation data but also provides an effective tool for reliability assessment in engineering practice.

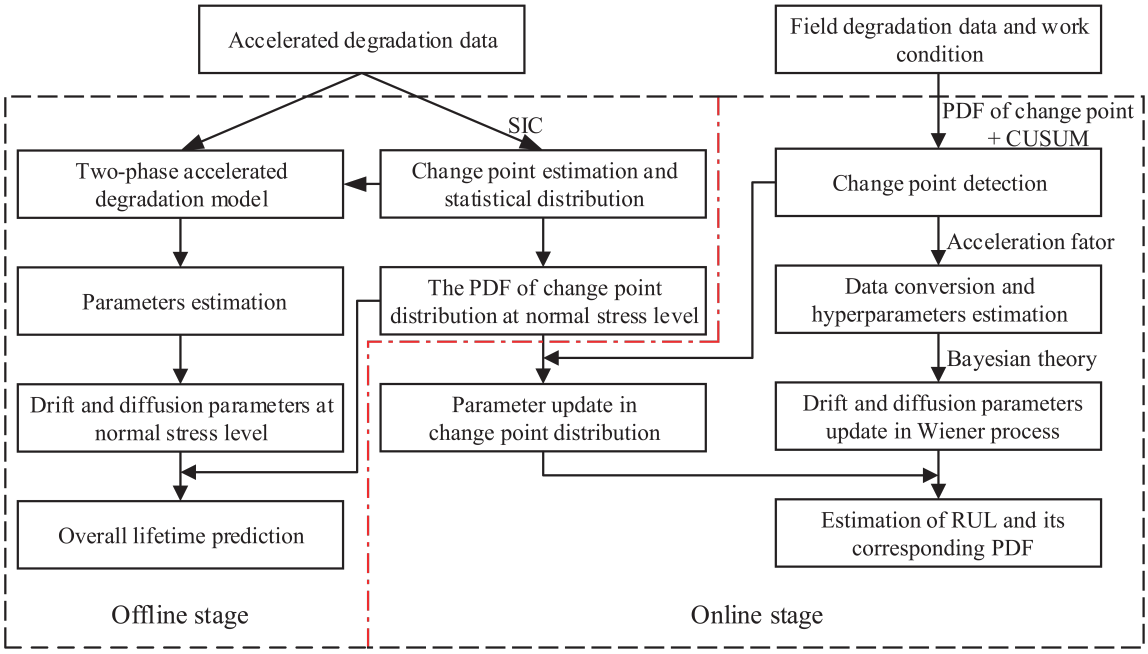

Figure 18. A flowchart of the proposed method in [17].

Zhang et al. [50] studied a RUL prediction model for the stator GI of generators, as shown in Figure 19. A digital twin-driven two-stage RUL prediction model was proposed, integrating both common and individual degradation information to improve the accuracy of RUL predictions for individual products. A digital twin framework was constructed, consisting of a common representation model (CRM), individual representation model (IRM), and dynamic evolution model, incorporating the Wiener process model, KF algorithm, and SVM model. Specifically, the CRM based on the two-stage Wiener process was developed to reflect the common characteristics of products. The CRM was used as the state equation, and the IRM based on KF was established to integrate individual degradation information and common degradation information of GI, reflecting the individual characteristics of a product. Additionally, SVM was employed to address the issue of covariance matrix updates in the KF algorithm for long-lifetime product predictions, enabling the dynamic evolution of the digital twin system. Experimental validation demonstrated the effectiveness and engineering applicability of the model. The results showed that, compared to using only the traditional Wiener process model, the digital twin model, which integrates field data, significantly improved prediction accuracy, reducing the relative prediction error from 6.16–16.07% to 2.90–5.27%. Moreover, the model that considered the two-stage degradation process and covariance matrix updates was

more effective in tracking the maximum PD values, resolving the gradual instability often encountered by the single-stage model in the second phase. By updating the covariance matrix using SVM, the model more accurately reflected field information, improving the prediction accuracy from 8.81–13.50% to 2.90–5.27%. Ultimately, experimental validation showed that the RUL prediction error ranged from 2.16% to 5.84%, proving that the digital twin model significantly enhances the accuracy of RUL prediction for generator GI and provides engineering guidance for generator operation and maintenance management.

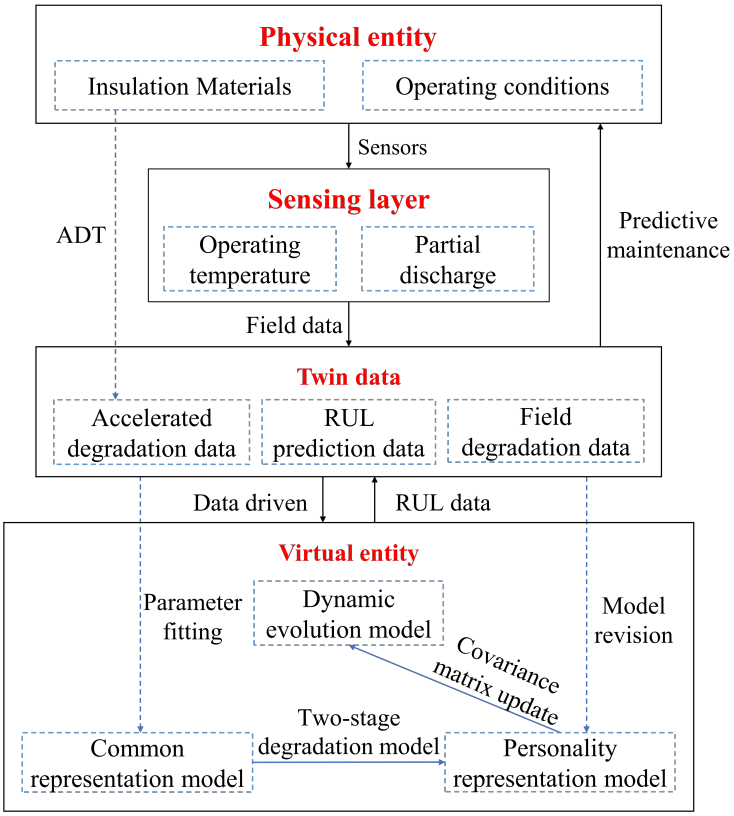

Figure 19. Structure of the digital-twin-driven RUL prediction model in [50].

5.4. Advantages and Limitations

The lifetime prediction model based on stochastic processes is highly interpretable, as its model parameters are closely related to the degradation and failure process of the product. This provides the model with good interpretability, such as degradation rate parameters that reflect the speed of degradation and diffusion coefficients that capture the time-varying uncertainty of the degradation process. Stochastic process-based lifetime modeling methods also offer flexibility and dynamic updating capabilities. The flexibility is evident in their ability to adapt to the complexity of various degradation paths, especially when the degradation behavior exhibits randomness and uncertainty. By utilizing techniques such as Bayesian updating, the model can dynamically adjust with new data, thus improving the timeliness and accuracy of predictions. In addition, stochastic process models not only provide point estimates of lifetime but also offer lifetime distributions and confidence intervals, which are helpful for reliability assessments.

However, the limitations of this approach should not be overlooked. On one hand, the parameter estimation of stochastic process models is highly dependent on the quantity and quality of the data. In particular, when experimental data are insufficient or noisy, the performance of the model may be compromised. On the other hand, to address more complex operating conditions of electrical machines, joint stochastic process modeling

under multiple stress conditions involves intricate mathematical derivations and numerical calculations, which impose high technical demands for practical applications. Furthermore, when the degradation process exhibits discontinuous characteristics, the applicability of existing stochastic process models may be limited. In summary, while stochastic process-based lifetime prediction models provide a powerful tool for handling lifetime data and predicting the remaining lifetime of products, their limitations must be overcome in practical applications to achieve more accurate lifetime predictions.

6. Potential Applications of Insulation Thermal Lifetime Models

Insulation thermal lifetime models provide an important theoretical basis for motor design, operation, maintenance, and standard development. By quantifying the impact of thermal stress on insulation performance, these models can assist engineers in predicting motor lifetime, optimizing design schemes, and developing efficient fault management strategies. This section explores the main application directions of insulation thermal lifetime models in practical engineering.

6.1. Reliability-Oriented Optimization Design for EMs

The application of insulation thermal lifetime models in engineering design optimization has been proven to be a key tool for improving motor performance and reliability [2,5,126]. Traditional over-engineering design methods often rely on increasing insulation thickness to ensure safety margins, but this can lead to a decrease in slot fill factor and power density. In contrast, reliability-oriented design (ROD) methods based on thermal lifetime models can optimize motor performance while ensuring reliability, thus alleviating the conflict between performance and reliability [2]. Modern design methods utilize accelerated thermal aging tests to obtain key data, which are then used to construct insulation lifetime models, such as the Arrhenius model or Arrhenius–Miner model. These models can serve as constraints in multi-objective optimization design, thereby optimizing both the reliability and performance of the motor. For example, in aerospace motor design, the model is used to predict the lifetime performance of different insulation schemes under high power density, thereby optimizing the selection of motor structure [126]. Furthermore, a ROD process, as shown in Figure 20, has been proposed in the literature [2], which integrates the PoF into the motor design framework, using statistical analysis and lifetime modeling methods to accurately assess the reliability of insulation systems. This method reduces the reliance on over-engineering while improving performance by incorporating reliability as part of the design objective. Additionally, in an automotive application case study, the connection between temperature, PD risk, and insulation thermal lifetime was used to determine the marginal hotspot temperature of windings, demonstrating the potential for enhancing motor performance through a deeper understanding of insulation degradation, and how ROD methods can improve motor power density [42]. This model-based optimization approach not only enhances the scientific basis of motor design but also significantly reduces experimental costs, providing a more economically feasible solution for high-performance motor design.

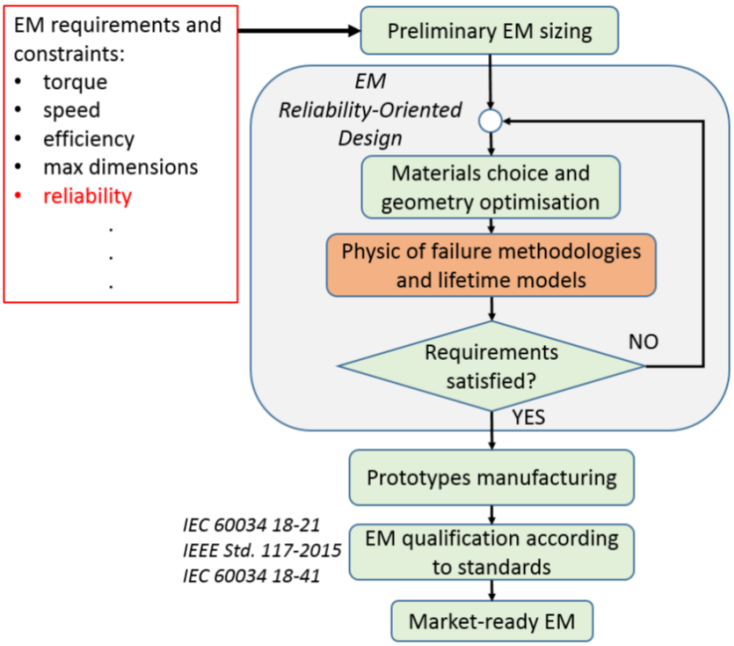

Figure 20. A flowchart of the reliability-oriented EM design proposed in [2,18,25,127].

6.2. Fault Prediction and Health Management

Insulation thermal lifetime models have immense potential in motor fault prediction and health management. The method proposed in [17,50], which integrates accelerated degradation data with field information, enables accurate RUL prediction for EMs in service by monitoring PD. By combining online monitoring data (such as temperature, current, voltage, and PD intensity), these models can assess the insulation condition of motors in real-time and predict the occurrence of faults, providing a basis for preventive maintenance. Unlike traditional experience-based maintenance methods, health management approaches based on thermal lifetime models offer more scientific and accurate predictions. For example, in the health management of industrial EMs, systems based on thermal lifetime models can predict the RUL of insulation materials through real-time monitoring and data analysis, enabling early maintenance actions to avoid sudden failures and prolonged downtime. In fields such as wind power generation and rail transportation, these models can significantly enhance motor reliability, reduce maintenance costs, and improve operational safety. Based on the accurate prediction of the failure time, these models also provide effective decision support for maintenance personnel, optimizing repair strategies and reducing maintenance cycles. Furthermore, by integrating big data technology and AI, health management systems based on thermal lifetime models can achieve an intelligent assessment of equipment status. By continually updating historical data, the model can self-adapt and ensure that predictive accuracy continuously improves. This data-driven intelligent health management approach demonstrates significant potential in enhancing motor operating efficiency and extending equipment lifetime.

6.3. Standard Development and Testing Method Improvement

Insulation thermal lifetime models play an essential role in the development of testing standards and methods for motor insulation systems. For non-impregnated windings, IEC 60034-18-41 provides testing standards and environmental enhancement factors for Type I insulation under PD risks [127]. However, there is a gap in standardized testing for impregnated samples. The study in [42] considered different wire sizes and insulation materials under thermal stress and validated the applicability of the proposed environmental factors, supplementing the IEC standards. These models provide quantitative evidence

that can optimize the design of ADTs, improving both the efficiency and reliability of the experimental results. Traditional ADTs often rely on experience or standardized test procedures, while thermal lifetime models can precisely determine the key parameters of these experiments, such as temperature, humidity, and aging time. By simulating the degradation process under various conditions, these models predict the lifetime of materials in real operational environments, offering more scientifically grounded testing methods and improving existing standardized testing procedures. For example, for EMs operating in high-temperature environments, the analysis based on thermal lifetime models can optimize the test temperature and duration, making the results more reflective of actual operating conditions and improving the reliability of experimental data. Furthermore, thermal lifetime models can be applied to the development of new insulation materials. With the continuous development of new materials, traditional testing methods may not be sufficient to evaluate these new materials' performance. Thermal lifetime models can provide performance predictions for different materials under specific thermal stresses, helping to develop more reasonable classification standards. For instance, models can help determine the degradation rates of various materials under different temperature conditions, thus providing a scientific basis for the application of new motor materials. For motors already in service, standardized tests based on thermal lifetime models can help maintenance personnel identify potential lifetime issues and issue early warnings. Additionally, these models can assess EMs' performance in extreme environments, providing a basis for the development of more comprehensive operational and maintenance standards.

6.4. Future Applications in Intelligent EM Systems

With the ability to accurately map physical entities to virtual space, digital twin technology has already achieved significant results in the state assessment and operation management of electromechanical systems. Venkatesan et al. [128] developed a digital twin system using a NN modeling approach to assess the health state of on-site motors based on runtime, vehicle distance, and motor health status. Wang et al. [129] proposed a health state evaluation method for robotic joints based on a five-dimensional digital twin model, using CNNs to predict stator currents and detect bearing faults. They also developed a visualization and operation and maintenance platform for robotic joints. Aivaliotis et al. [130] 2019] used a physics-based digital twin simulation approach to calculate the remaining service life of mechanical equipment for predictive maintenance. Li et al. [131] summarized key manufacturing technologies based on digital twins for the life cycle of aircraft engine spindle bearings, along with fault diagnosis and life analysis. Xiong et al. [132] proposed a digital twin-driven predictive maintenance framework for aircraft engines, developing an implicit digital twin model to predict the RUL of aircraft engines. As the Internet of Things (IoT) and AI technologies continue to evolve, the potential applications of insulation thermal lifetime models in intelligent EM systems will expand significantly. For example, in the field of smart manufacturing, these models can be integrated with digital twin technology to enable precise management of the EM's entire life cycle. By updating models with real-time monitoring data, digital twin systems can dynamically assess insulation status and optimize operating strategies. Furthermore, thermal lifetime models can be embedded into motor control systems as a basis for optimizing operational parameters. For example, load management algorithms based on lifetime models can adjust power output in real-time to minimize the impact of thermal stress on the insulation system, thereby extending the service life of the equipment.

7. Conclusions

This review paper systematically examines the methods for lifetime assessment and prediction of EIS under thermal aging, with a focus on the application of different approaches such as PoF-based models, data-driven models, and stochastic process models in insulation lifetime modeling. With the continuous development of EM technology, the reliability requirements for EIS have become increasingly demanding, particularly under high power density, high temperatures, and complex operating conditions. Insulation aging has become a key factor limiting both the lifetime and performance of EMs. By conducting thermal aging tests and establishing lifetime models, engineers can more accurately predict the lifetime of insulation materials, optimize design schemes, and enhance the reliability and cost-effectiveness of electrical machines.

Firstly, PoF-based lifetime modeling methods provide a scientific basis for understanding the aging mechanisms of insulation materials. By considering the effects of thermal stress, these models can accurately describe the thermal aging and damage of insulation. However, these models still face certain challenges when applied to multi-physics field coupling and complex operating conditions. Secondly, data-driven methods, particularly NN algorithms and CF techniques, utilize ADT data to efficiently capture complex nonlinear relationships. These methods exhibit strong predictive capabilities, but their dependence on high-quality data and the lack of interpretability remain significant limitations. Furthermore, stochastic process-based lifetime modeling methods provide effective tools for accounting for the randomness and uncertainty in the degradation process, especially in describing the irreversibility and random fluctuations of thermal aging in insulation materials.

This review also explores the potential applications of thermal lifetime models in areas such as EM design optimization, fault prediction and health management, as well as standard development and test method improvements. By integrating thermal lifetime models, designers can optimize insulation design while ensuring machine performance and extend the lifetime of EMs. Additionally, by combining real-time monitoring data, thermal lifetime models can effectively support fault prediction and health management, reducing the risk of failures and improving maintenance efficiency. Moreover, these models provide theoretical support for the development of scientific test standards and material evaluation methods, promoting the application of new insulation materials and the improvement of standardized testing procedures.

Despite the broad application prospects of thermal lifetime models in EM design and maintenance, challenges remain. These include issues related to multi-physics field coupling, the adaptability of models under complex operating conditions, and difficulties in acquiring and validating experimental data. Therefore, future research should continue to focus on integrating and optimizing different methods, promoting the development of intelligent EM systems based on thermal lifetime models, particularly through the integration of digital twin technologies, real-time data monitoring, and adaptive prediction models. In conclusion, the research and application of thermal lifetime models provide new perspectives and tools for reliability analysis, design optimization, and maintenance management of EM systems. As related technologies continue to develop, the application of these models in the EM industry will deepen, contributing to improved machine reliability, extended lifetimes, and the promotion of green intelligent manufacturing.

Author Contributions: Conceptualization, J.Z. and J.W. (Jianwei Wu); writing—original draft preparation, J.W. (Jiajin Wang); writing—review and editing, J.Z. and J.W. (Jiajin Wang); formal analysis, Q.Z.; investigation, J.W. (Jiajin Wang) and H.L.; methodology, J.W. (Jianwei Wu); supervision, C.M. and Y.F.; Project administration, X.H. (Xiangning He) and X.H. (Xiaoyan Huang); funding acquisition, J.Z. and H.L. All authors have read and agreed to the published version of the manuscript.

Funding: This work was supported by Key Project of the State Key Laboratory of Fluid Power and Mechatronic Systems SKLoFP_ZZ_2405, the Key Research and Development Program of Zhejiang Province under Grant 2024C01140, the Key Research and Development Program of Hangzhou under Grant 2024SZD1A18, and A Project Supported by Scientific Research Fund of Zhejiang University (XY2024016).

Conflicts of Interest: Author Hongbo Li was employed by the company Zhejiang Guoli Security Technology Co., LTD.. The remaining authors declare that the research was conducted in the absence of any commercial or financial relationships that could be construed as a potential conflict of interest.

Abbreviations

The following abbreviations are used in this manuscript:

EM	Electrical Machine
EIS	Electrical Insulation System
CR	Corona-Resistant
ALT	Accelerated Lifetime Test
ADT	Accelerated Degradation Test
PoF	Physics of Failure
AI	Artificial Intelligence
GI	Groundwall Insulation
IR	Insulation Resistance
PD	Partial Discharge
RBV	Residual Breakdown Voltage
BV	Breakdown Voltage
IC	Insulation Capacitance
PDIV	Partial-Discharge Inception Voltage
PDEV	Partial-Discharge Extinction Voltage
SEM	Scanning Electron Microscopy
FTIR	Fourier Transform Infrared Spectroscopy
TGA	Thermogravimetric Analysis
OCT	Optical Coherence Tomography
DSC	Differential Scanning Calorimeter
CDF	Cumulative Distribution Function
PCA	Principal Component Analysis
NN	Neural Network
SVM	Support Vector Machine
RF	Random Forest
ANN	Artificial Neural Network
RBFG	Radial Basis Function Gaussian
ROM	Random Optimization Method
LM	Levenberg–Marquardt
BP	Back Propagation
LSM	Least-Squares Method
LSTM	Long Short-Term Memory
RNN	Recurrent Neural Network
BRP	Bayesian Regularized Back Propagation
CF	Curve Fitting
MTTF	Mean Time-to-Failure
FPT	First Passage Time
PDF	Probability Density Function
RUL	Remaining Useful Lifetime
EM	Expectation–Maximization
SIC	Schwarz Information Criterion
KF	Kalman Filtering

CFD	Computational Fluid Dynamics
SCARA	Selective Compliance Assembly Robot Arm
PMSM	Permanent Magnet Synchronous Motors
RSSMC	Residual Sum of Squares Minimum Criterion
CUSUM	Cumulative Sum Control Chart
CRM	Common Representation Model
IRM	Individual Representation Model
ROD	Reliability-Oriented Design
IoT	Internet of Things

References

1. *IEC 60505:2011*; Evaluation and Qualification of Electrical Insulation Systems. International Electrotechnical Commissio: Geneva, Switzerland, 2011.
2. Giangrande, P.; Madonna, V.; Nuzzo, S.; Galea, M. Moving toward a reliability-oriented design approach of low-voltage electrical machines by including insulation thermal aging considerations. *IEEE Trans. Transp. Electrif.* **2020**, *6*, 16–27.
3. Madonna, V.; Giangrande, P.; Lusuardi, L.; Cavallini, A.; Gerada, C.; Galea, M. Thermal overload and insulation aging of short duty cycle, aerospace motors. *IEEE Trans. Ind. Electron.* **2019**, *67*, 2618–2629.
4. Fernando, M.; Naranpanawa, W.; Rathnayake, R.; Jayantha, G. Condition assessment of stator insulation during drying, wetting and electrical ageing. *IEEE Trans. Dielectr. Electr. Insul.* **2013**, *20*, 2081–2090.
5. Ji, Y.; Giangrande, P.; Madonna, V.; Zhao, W.; Galea, M. Reliability-oriented design of inverter-fed low-voltage electrical machines: Potential solutions. *Energies* **2021**, *14*, 4144.
6. Han, J.; Liu, X.; Shao, X.; Nie, L.; Jin, H.; Huang, X. Residual Breakdown Field Strength Prediction of Stator Bar Insulation of Pumped Storage Generator Based on SVM. In Proceedings of the 2022 4th International Conference on Power and Energy Technology (ICPET), Beijing, China, 28–31 July 2022; IEEE: Piscataway, NJ, USA, 2022; pp. 187–192.
7. Lee, H.; Kim, H.; Jeong, J.; Lee, K.; Lee, S.B.; Stone, G.C. Inverter-embedded partial discharge testing for reliability enhancement of stator winding insulation in low voltage machines. *IEEE Trans. Ind. Appl.* **2022**, *58*, 2088–2096.
8. Kim, Y.; Nelson, J. Assessment of deterioration in epoxy/mica machine insulation. *IEEE Trans. Electr. Insul.* **1992**, *27*, 1026–1039.
9. Tanaka, K.; Kojima, H.; Onoda, M.; Suzuki, K. Prediction of residual breakdown electrical field strength of epoxy-mica paper insulation systems for the stator winding of large generators. *IEEE Trans. Dielectr. Electr. Insul.* **2015**, *22*, 1118–1123.
10. Riba, J.R.; Moreno-Eguilaz, M.; Bogarra, S. Tracking Resistance in Polymeric Insulation Materials for High-Voltage Electrical Mobility Applications Evaluated by Existing Test Methods: Identified Research Needs. *Polymers* **2023**, *15*, 3717.
11. Kong, X.; Zhang, C.; Du, H.; Miyake, H.; Tanaka, Y.; Du, B. Effects of Thermo-oxidative Aging on the Dielectric Property and Electrical Breakdown of Epoxy Resin Using in High Voltage Equipment. *IEEE Trans. Dielectr. Electr. Insul.* **2024**. Doi: 10.1109/TDEI.2024.3501997.
12. Li, L.; Guan, C.; Zhang, A.; Chen, D.; Qing, Z. Thermal stabilities and the thermal degradation kinetics of polyimides. *Polym. Degrad. Stab.* **2004**, *84*, 369–373.
13. Yang, Y.; Yin, D.; Xiong, R.; Shi, J.; Tian, F.; Wang, X.; Lei, Q. Ftir and dielectric studies of electrical aging in polyimide under AC voltage. *IEEE Trans. Dielectr. Electr. Insul.* **2012**, *19*, 574–581.
14. Huang, X.; Li, Q.; Liu, T.; Han, S.; Lu, Y.; Wang, Z. Research on Kapton aerobic pyrolysis by using ReaxFF molecular dynamics simulation. In Proceedings of the 2016 IEEE International Conference on High Voltage Engineering and Application (ICHVE), Chengdu, China, 19–22 September 2016; IEEE: Piscataway, NJ, USA, 2016; pp. 1–5.
15. Wu, G.; Wu, J.; Zhou, L.; Gao, B.; Zhou, K.; Guo, X.; Cao, K. Microscopic view of aging mechanism of polyimide film under pulse voltage in presence of partial discharge. *IEEE Trans. Dielectr. Electr. Insul.* **2010**, *17*, 125–132.
16. Yang, Y.; Yin, D.; Zhong, C.; Xiong, R.; Shi, J.; Liu, Z.; Wang, X.; Lei, Q. Surface morphology and raman analysis of the polyimide film aged under bipolar pulse voltage. *Polym. Eng. Sci.* **2013**, *53*, 1536–1541.
17. Wang, J.; Wu, J.; Zhang, J.; Zhang, Q.; Fang, Y.; Huang, X. Remaining useful life prediction method by integrating two-phase accelerated degradation data and field information. *IEEE Trans. Instrum. Meas.* **2024**, *73*, 1–17.
18. *IEC 60034-18-21*; Rotating Electrical Machines—Part 18–21: Functional Evaluation of Insulation Systems—Test Procedures for Wire-Wound Windings— Thermal Evaluation and Classification. International Electrotechnical Commissio: Geneva, Switzerland, 2012.
19. Khowja, M.R.; Turabee, G.; Giangrande, P.; Madonna, V.; Cosma, G.; Vakil, G.; Gerada, C.; Galea, M. Lifetime estimation of enameled wires under accelerated thermal aging using curve fitting methods. *IEEE Access* **2021**, *9*, 18993–19003.
20. Han, C. Lifetime evaluation of class E electrical insulation for small induction motors. *IEEE Electr. Insul. Mag.* **2011**, *27*, 14–19.
21. Madonna, V.; Giangrande, P.; Migliazza, G.; Buticchi, G.; Galea, M. A time-saving approach for the thermal lifetime evaluation of low-voltage electrical machines. *IEEE Trans. Ind. Electron.* **2019**, *67*, 9195–9205.

22. Zhang, J.; Zhang, Q.; Huang, X.; Fang, Y.; Tian, J. Motor Insulation Remaining Useful Life Prediction Method Based on Accelerating Degradation Data and Field Degradation Data. *Trans. China Electrotech. Soc.* **2023**, *38*, 599–609. (In Chinese)
23. Stone, G.C.; Culbert, I.; Boulter, E.A.; Dhirani, H. *Electrical Insulation for Rotating Machines: Design, Evaluation, Aging, Testing, and Repair*; John Wiley & Sons: Hoboken, NJ, USA, 2014; Volume 83.
24. Griffo, A.; Tsyokhla, I.; Wang, J. Lifetime of machines undergoing thermal cycling stress. In Proceedings of the 2019 IEEE Energy Conversion Congress and Exposition (ECCE), Baltimore, MD, USA, 29 September–3 October 2019; IEEE: Piscataway, NJ, USA, 2019; pp. 3831–3836.
25. *IEEE Std 1310-2012 (Revision of IEEE Std 1310-1996)*; IEEE Recommended Practice for Thermal Cycle Testing of Form-Wound Stator Bars and Coils for Large Rotating Machines. IEEE: Piscataway, NJ, USA, 2012.
26. *IEC 60034-18-34*; Rotating Electrical Machines: Functional Evaluation of Insulation Systems: Test Procedures for Form-Wound Windings—Evaluation of Thermomechanical Endurance of Insulation Systems. International Electrotechnical Commissio: Geneva, Switzerland, 2012.
27. Kokko, V.I. Ageing due to thermal cycling by start and stop cycles in lifetime estimation of hydroelectric generator stator windings. In Proceedings of the 2011 IEEE International Electric Machines & Drives Conference (IEMDC), Niagara Falls, ON, Canada, 15–18 May 2011; IEEE: Piscataway, NJ, USA, 2011; pp. 318–323.
28. Mitsui, H.; Yoshida, K.; Inoue, Y.; Kenjo, S. Thermal cyclic degradation of coil insulation for rotating machines. *IEEE Trans. Power Appar. Syst.* **1983**, *PAS-102*, 67–73.
29. Zhou, X.; Ji, Y.; Giangrande, P.; Zhao, W.; Ijaz, S.; Galea, M. Extra Life Loss of Low Voltage Electrical Machine under Variable Temperature Aging. *IEEE Trans. Transp. Electrif.* **2024**. Doi: 10.1109/TTE.2024.3505923.
30. *IEC 60216-1:1990*; Guide for the Determination of Thermal Endurance Properties of Electrical Insulating Materials: Part 1: General Guidelines for Aging Procedures and Evaluation of Test Results. International Electrotechnical Commissio: Geneva, Switzerland, 1990.
31. Bhumiwat, S.A. Depolarization index for dielectric aging indicator of rotating machines. *IEEE Trans. Dielectr. Electr. Insul.* **2015**, *22*, 3126–3132.
32. Farahani, M.; Borsi, H.; Gockenbach, E. Study of capacitance and dissipation factor tip-up to evaluate the condition of insulating systems for high voltage rotating machines. *Electr. Eng.* **2007**, *89*, 263–270.
33. Emery, F. Partial discharge, dissipation factor, and corona aspects for high voltage electric generator stator bars and windings. *IEEE Trans. Dielectr. Electr. Insul.* **2005**, *12*, 347–361.
34. Farahani, M.; Borsi, H.; Gockenbach, E.; Kaufhold, M. Partial discharge and dissipation factor behavior of model insulating systems for high voltage rotating machines under different stresses. *IEEE Electr. Insul. Mag.* **2005**, *21*, 5–19.
35. Grubic, S.; Aller, J.M.; Lu, B.; Habetler, T.G. A survey on testing and monitoring methods for stator insulation systems of low-voltage induction machines focusing on turn insulation problems. *IEEE Trans. Ind. Electron.* **2008**, *55*, 4127–4136.
36. Werynski, P.; Roger, D.; Corton, R.; Brudny, J.F. Proposition of a new method for in-service monitoring of the aging of stator winding insulation in AC motors. *IEEE Trans. Energy Convers.* **2006**, *21*, 673–681.
37. Yang, J.; Cho, J.; Lee, S.B.; Yoo, J.Y.; Kim, H.D. An advanced stator winding insulation quality assessment technique for inverter-fed machines. *IEEE Trans. Ind. Appl.* **2008**, *44*, 555–564.
38. Savin, S.; Ait-Amar, S.; Roger, D. Turn-to-turn capacitance variations correlated to PDIV for AC motors monitoring. *IEEE Trans. Dielectr. Electr. Insul.* **2013**, *20*, 34–41.
39. Cavallini, A. Reliability of low voltage inverter-fed motors: What have we learned, perspectives, open points. In Proceedings of the 2017 International Symposium on Electrical Insulating Materials (ISEIM), Toyohashi, Japan, 11–15 September 2017; IEEE: Piscataway, NJ, USA, 2017; Volume 1, pp. 13–22.
40. Wang, P.; Xu, H.; Wang, J.; Cavallini, A.; Montanari, G.C. Temperature effects on PD statistics and endurance of inverter-fed motor insulation under repetitive square wave voltages. In Proceedings of the 2016 IEEE Electrical Insulation Conference (EIC), Montreal, QC, Canada, 19–22 June 2016; IEEE: Piscataway, NJ, USA, 2016; pp. 202–205.
41. Rumi, A.; Marinelli, J.; Cavallini, A. Towards the 2 nd edition of IEC 60034-18-41: Challenges and perspectives. In Proceedings of the 2021 3rd International Conference on High Voltage Engineering and Power Systems (ICHVEPS), Bandung, Indonesia, 5–6 October 2021; IEEE: Piscataway, NJ, USA, 2021; pp. 052–056.
42. Ji, Y.; Giangrande, P.; Zhao, W.; Madonna, V.; Zhang, H.; Galea, M. Determination of hotspot temperature margin for rectangular wire windings considering insulation thermal degradation and partial discharge. *IEEE Trans. Transp. Electrif.* **2023**, *10*, 2057–2069.
43. Naderiallaf, H.; Degano, M.; Gerada, C. PDIV modelling for rectangular wire turn-to-turn insulation of inverter-fed motors through thermal ageing. *IEEE Trans. Dielectr. Electr. Insul.* **2023**, *31*, 550–559.
44. Madonna, V.; Giangrande, P.; Galea, M. Evaluation of strand-to-strand capacitance and dissipation factor in thermally aged enamelled coils for low-voltage electrical machines. *IET Sci. Meas. Technol.* **2019**, *13*, 1170–1177.
45. Zhe, H. Modeling and Testing of Insulation Degradation due to Dynamic Thermal Loading of Electrical Machines. Ph.D Thesis, Lund University, Lund, Sweden, 2017.

46. Gyftakis, K.N.; Sumislawska, M.; Kavanagh, D.F.; Howey, D.A.; McCulloch, M.D. Dielectric characteristics of electric vehicle traction motor winding insulation under thermal aging. *IEEE Trans. Ind. Appl.* **2015**, *52*, 1398–1404.
47. Farahani, M.; Gockenbach, E.; Borsi, H.; Schäfer, K.; Kaufhold, M. Behavior of machine insulation systems subjected to accelerated thermal aging test. *IEEE Trans. Dielectr. Electr. Insul.* **2010**, *17*, 1364–1372.
48. Khowja, M.R.; Vakil, G.; Ahmad, S.S.; Ramanathan, R.; Gerada, C.; Benarous, M. Life Characterisation of PEEK and Nanofilled Enamel Insulated Wires under Thermal Ageing. *IEEE Access* **2024**, *12*, 39470–39483.
49. Gyftakis, K.N.; Panagiotou, P.; Lophitis, N.; Howey, D.A.; McCulloch, M.D. Breakdown resistance analysis of traction motor winding insulation under thermal ageing. In Proceedings of the 2017 IEEE Energy Conversion Congress and Exposition (ECCE), Cincinnati, OH, USA, 1–5 October 2017; IEEE: Piscataway, NJ, USA, 2017; pp. 5819–5825.
50. Zhang, Q.; Wu, J.; Wang, J.; Huang, X.; Fang, Y.; Niu, F.; Zhang, J. A Two-phase Lifetime Prediction Model of Generator Stator Main Wall Insulation Driven by Digital Twin. *IEEE Trans. Instrum. Meas.* **2024**, *73*, 1–12.
51. Wang, J.; Xu, L.; Cai, L.; Zhang, J.; Tian, J. CFD-based Temperature Field Analysis and Lifetime Prediction of Brushless DC Motor. In Proceedings of the 2022 IEEE Transportation Electrification Conference and Expo, Asia-Pacific (ITEC Asia-Pacific), Haining, China, 28–31 October 2022; IEEE: Piscataway, NJ, USA, 2022; pp. 1–5.
52. Liao, R.; Tang, C.; Yang, L. Research on the microstructure and morphology of power transformer insulation paper after thermal aging. *Proc. Chin. Soc. Electr. Eng.* **2007**, *27*, 59. (In Chinese)
53. Mezgebo, B.; Sherif, S.S.; Fernando, N.; Kordi, B. Paper Insulation Aging Estimation Using Swept-Source Optical Coherence Tomography. *IEEE Trans. Dielectr. Electr. Insul.* **2022**, *29*, 30–37.
54. Zhou, L.; Liu, C.; Quan, S.; Zhang, X.; Wang, D. Experimental study on ageing characteristics of electric locomotive ethylene propylene rubber cable under mechanical–thermal combined action. *High Volt.* **2022**, *7*, 792–801.
55. Xie, Q. AFM analysis and fractal feature extraction of epoxy resin after surface flashover. *Trans. China Electrotech. Soc* **2017**, *32*, 245–254. (In Chinese)
56. Hsu, Y.; Chang-Liao, K.; Wang, T.; Kuo, C. Monitoring the moisture-related degradation of ethylene propylene rubber cable by electrical and SEM methods. *Polym. Degrad. Stab.* **2006**, *91*, 2357–2364.
57. Hao, Y.; Xie, H. Degradation Behavior of Stator Insulation for Large Generators Using X-Ray Diffraction Method. *Trans. China Electrotech. Soc.* **2007**, *22*, 16–21. (In Chinese)
58. Zheng, Z.; Lu, B.; Gan, W.; Huang, Z.; Li, J.; Wang, F.; Li, S.Q.; Wang, Q. Aging Characterization of Oil-paper Insulation Based on Fluorescence Characteristics of Suspended Fibers in Oil. *IEEE Trans. Dielectr. Electr. Insul.* **2024**, *31*, 3405–3413.
59. Popescu, M.; Staton, D.A.; Boglietti, A.; Cavagnino, A.; Hawkins, D.; Goss, J. Modern heat extraction systems for power traction machines—A review. *IEEE Trans. Ind. Appl.* **2016**, *52*, 2167–2175.
60. Kokko, V.I. Electrical ageing in lifetime estimation of hydroelectric generator stator windings. In Proceedings of the XIX International Conference on Electrical Machines-ICEM 2010, Rome, Italy, 6–8 September 2010; IEEE: Piscataway, NJ, USA, 2010; pp. 1–5.
61. Montanari, G.C.; Simoni, L. Aging phenomenology and modeling. *IEEE Trans. Electr. Insul.* **1993**, *28*, 755–776.
62. Dakin, T.W. Electrical insulation deterioration treated as a chemical rate phenomenon. *Trans. Am. Inst. Electr. Eng.* **1948**, *67*, 113–122.
63. Sciascera, C.; Galea, M.; Giangrande, P.; Gerada, C. Lifetime consumption and degradation analysis of the winding insulation of electrical machines. In Proceedings of the 8th IET International Conference on Power Electronics, Machines and Drives (PEMD 2016), Glasgow, UK, 19–21 April 2016; IET: Stevenage, UK, 2016; pp. 1–5.
64. Gnacinski, P. Windings temperature and loss of life of an induction machine under voltage unbalance combined with over-or undervoltages. *IEEE Trans. Energy Convers.* **2008**, *23*, 363–371.
65. Movahed, S.; Mirzamani, S.O.; Rajabi, A.; Daneshvar, H. Estimation of insulation life of inverter-fed induction motors. In Proceedings of the 2010 1st Power electronic & drive systems & technologies conference (PEDSTC), Tehran, Iran, 17–18 February 2010; IEEE: Piscataway, NJ, USA, 2010; pp. 335–339.
66. Kulan, M.C.; Baker, N.J. Life-time characteristics of random wound compressed stator windings under thermal stress. *IET Electr. Power Appl.* **2019**, *13*, 1287–1297.
67. Rahnamaei, S.R.; Nejad, S.M.S.; Rashidi, A.; Sohankar, A. Dynamic thermal model for winding temperature of an SRM in an integrated battery charger utilized in electric vehicles. *IEEE Trans. Energy Convers.* **2020**, *36*, 1766–1775.
68. Huang, Z.; Márquez-Fernández, F.J.; Loayza, Y.; Reinap, A.; Alaküla, M. Dynamic thermal modeling and application of electrical machine in hybrid drives. In Proceedings of the 2014 international conference on electrical machines (ICEM), IEEE: Piscataway, NJ, USA, 2014, pp. 2158–2164.
69. *IEC 60317-0-1*; Specifications for Particular Types of Winding Wires—Part 0–1: General Requirements—Enamelled Round Copper Wire. International Electrotechnical Commissio: Geneva, Switzerland, 2013.
70. Feilat, E.A. Lifetime assessment of electrical insulation. In *Electric Field*; IntechOpen: London, UK, 2018.

71. Mancinelli, P.; Stagnitta, S.; Cavallini, A. Qualification of hairpin motors insulation for automotive applications. *IEEE Trans. Ind. Appl.* **2016**, *53*, 3110–3118.
72. Du, S.; Huang, Z.; Jin, L.; Wan, X. Recent Progress in Data-Driven Intelligent Modeling and Optimization Algorithms for Industrial Processes. *Algorithms* **2024**, *17*, 569.
73. Zahra, S.T.; Imdad, S.K.; Khan, S.; Khalid, S.; Baig, N.A. Power transformer health index and life span assessment: A comprehensive review of conventional and machine learning based approaches. *Eng. Appl. Artif. Intell.* **2025**, *139*, 109474.
74. Gupta, T.K.; Raza, K. Optimization of ANN architecture: A review on nature-inspired techniques. In *Machine Learning in Bio-Signal Analysis and Diagnostic Imaging*; Academic Press: Cambridge, MA, USA, 2019; pp. 159–182.
75. Turabee, G.; Khowja, M.R.; Giangrande, P.; Madonna, V.; Cosma, G.; Vakil, G.; Gerada, C.; Galea, M. The role of neural networks in predicting the thermal life of electrical machines. *IEEE Access* **2020**, *8*, 40283–40297.
76. Mokhnache, L.; Boubakeur, A.; Noureddine, B.O.; Bedja, M.; Feliachi, A. Application of Neural networks in the thermal ageing prediction of transformer oil. In Proceedings of the 2001 Power Engineering Society Summer Meeting. Conference Proceedings (Cat. No. 01CH37262), Vancouver, BC, Canada, 15–19 July 2001; IEEE: Piscataway, NJ, USA, 2001; Volume 3, pp. 1865–1868.
77. Mokhnache, L.; Boubakeur, A.; Said, N.N. Application of neural networks paradigms in the diagnosis and thermal ageing prediction of transformer oil. In Proceedings of the 2002 IEEE 14th International Conference on Dielectric Liquids, ICDL 2002 (Cat. No. 02CH37319), Graz, Austria, 12 July 2002; IEEE: Piscataway, NJ, USA, 2002; pp. 258–261.
78. Mokhnache, L.; Boubakeur, A.; Said, N.N. Comparison of different neural networks algorithms used in the diagnosis and thermal ageing prediction of transformer oil. In Proceedings of the IEEE International Conference on Systems, Man and Cybernetics, Yasmine Hammamet, Tunisia, 6–9 October 2002; IEEE: Piscataway, NJ, USA, 2002, Volume 6.
79. Mokhnache, L.; Verma, P.; Boubakeur, A. Neural networks in prediction of accelerated thermal ageing effect on oil/paper insulation tensile strength. In Proceedings of the 2004 IEEE International Conference on Solid Dielectrics—ICSD 2004, Toulouse, France, 5–9 July 2004; IEEE: Piscataway, NJ, USA, 2004; Volume 2, pp. 575–577.
80. Mokhnache, L.; Boubakeur, A. Prediction of the breakdown voltage in a point-barrier-plane air gap using neural networks. In Proceedings of the 2001 Annual Report Conference on Electrical Insulation and Dielectric Phenomena (Cat. No. 01CH37225), Kitchener, ON, Canada, 14–17 October 2001; IEEE: Piscataway, NJ, USA, 2001; pp. 369–372.
81. Mokhnache, L.; Boubakeur, A. The use of some paradigms of neural networks in prediction of dielectric properties for high voltage liquid solid and gas insulations. In Proceedings of the Conference Record of the the 2002 IEEE International Symposium on Electrical Insulation (Cat. No. 02CH37316), Boston, MA, USA, 7–10 April 2002; IEEE: Piscataway, NJ, USA, 2002; pp. 306–309.
82. Boukezzi, L.; Boubakeur, A. Prediction of mechanical properties of XLPE cable insulation under thermal aging: Neural network approach. *IEEE Trans. Dielectr. Electr. Insul.* **2013**, *20*, 2125–2134.
83. Boukezzi, L.; Boubakeur, A. Comparison of some neural network algorithms used in prediction of XLPE HV insulation properties under thermal aging. In Proceedings of the 2012 IEEE International Conference on Condition Monitoring and Diagnosis, Bali, Indonesia, 23–27 September 2012; IEEE: Piscataway, NJ, USA, 2012, pp. 1218–1222.
84. Zhao, J.X.; Jin, H.Z.; Han, H.W. Dielectric loss factor forecasting based on artificial neural network. In Proceedings of the 2009 Second International Conference on Information and Computing Science, Manchester, UK, 21–22 May 2009; IEEE: Piscataway, NJ, USA, 2009; Volume 3, pp. 177–180.
85. Shprekher, D.; Babokin, G.; Kolesnikov, E. Application of neural networks for prediction of insulation condition in networks with isolated neutral. In Proceedings of the 2019 International Russian Automation Conference (RusAutoCon), Sochi, Russia, 8–14 September 2019; IEEE: Piscataway, NJ, USA, 2019; pp. 1–6.
86. Turabee, G.; Cosma, G.; Madonna, V.; Giangrande, P.; Khowja, M.R.; Vakil, G.; Gerada, C.; Galea, M. Predicting insulation resistance of enamelled wire using neural network and curve fit methods under thermal aging. In Proceedings of the 2020 International Joint Conference on Neural Networks (IJCNN), Glasgow, UK, 19–24 July 2020; IEEE: Piscataway, NJ, USA, 2020; pp. 1–7.
87. Ye, Z.S.; Wang, Y.; Tsui, K.L.; Pecht, M. Degradation data analysis using Wiener processes with measurement errors. *IEEE Trans. Reliab.* **2013**, *62*, 772–780.
88. Hou, Y.; Du, Y.; Peng, Y.; Liu, D. An improved random effects Wiener process accelerated degradation test model for lithium-ion battery. *IEEE Trans. Instrum. Meas.* **2021**, *70*, 1–11.
89. Chen, M.; Zhang, B.; Li, H.; Gao, X.; Wang, J.; Zhang, J. Lifetime Prediction of Permanent Magnet Synchronous Motor in Selective Compliance Assembly Robot Arm Considering Insulation Thermal Aging. *Sensors* **2024**, *24*, 3747.
90. Van Noortwijk, J.M. A survey of the application of gamma processes in maintenance. *Reliab. Eng. Syst. Saf.* **2009**, *94*, 2–21.
91. Zhao, S.; Peng, Y.; Yang, F.; Ugur, E.; Akin, B.; Wang, H. Health state estimation and remaining useful life prediction of power devices subject to noisy and aperiodic condition monitoring. *IEEE Trans. Instrum. Meas.* **2021**, *70*, 1–16.
92. Wang, H.; Xu, T.; Mi, Q. Lifetime prediction based on Gamma processes from accelerated degradation data. *Chin. J. Aeronaut.* **2015**, *28*, 172–179.
93. Abdel-Hameed, M. A gamma wear process. *IEEE Trans. Reliab.* **1975**, *24*, 152–153.

94. Singpurwalla, N.D. Survival in dynamic environments. *Stat. Sci.* **1995**, *10*, 86–103.
95. Park, C.; Padgett, W. Accelerated degradation models for failure based on geometric Brownian motion and gamma processes. *Lifetime Data Anal.* **2005**, *11*, 511–527.
96. Lawless, J.; Crowder, M. Covariates and random effects in a gamma process model with application to degradation and failure. *Lifetime Data Anal.* **2004**, *10*, 213–227.
97. Mahmoodian, M.; Alani, A. Modeling deterioration in concrete pipes as a stochastic gamma process for time-dependent reliability analysis. *J. Pipeline Syst. Eng. Pract.* **2014**, *5*, 04013008.
98. Wei, Q.; Xu, D. Remaining useful life estimation based on gamma process considered with measurement error. In Proceedings of the 2014 10th International Conference on Reliability, Maintainability and Safety (ICRMS), Guangzhou, China, 6–8 August 2014; IEEE: Piscataway, NJ, USA, 2014, pp. 645–649.
99. Park, S.H.; Kim, J.H. Application of gamma process model to estimate the lifetime of photovoltaic modules. *Sol. Energy* **2017**, *147*, 390–398.
100. Park, S.H.; Kim, J.H. Lifetime estimation of LED lamp using gamma process model. *Microelectron. Reliab.* **2016**, *57*, 71–78.
101. Bhattacharyya, G.; Fries, A. Fatigue Failure Models - Birnbaum-Saunders vs. Inverse Gaussian. *IEEE Trans. Reliab.* **1982**, *31*, 439–441.
102. Doksum, K.A.; Hbyland, A. Models for variable-stress accelerated life testing experiments based on wener processes and the inverse gaussian distribution. *Technometrics* **1992**, *34*, 74–82.
103. Guérin, F.; Barreau, M.; Cloupet, S.; Hersant, J.; Hambli, R. Bayesian estimation of degradation model defined by a Wiener process-Application on disc brake wear. *IFAC Proc. Vol.* **2010**, *43*, 74–79.
104. Çağlar, R.; İkizoğlu, S.; Şeker, S. Statistical Wiener process model for vibration signals in accelerated aging processes of electric motors. *J. Vibroengineering* **2014**, *16*, 800–807.
105. Whitmore, G. Estimating degradation by a Wiener diffusion process subject to measurement error. *Lifetime Data Anal.* **1995**, *1*, 307–319.
106. Wang, X. Wiener processes with random effects for degradation data. *J. Multivar. Anal.* **2010**, *101*, 340–351.
107. Si, X.S.; Wang, W.; Hu, C.H.; Zhou, D.H.; Pecht, M.G. Remaining useful life estimation based on a nonlinear diffusion degradation process. *IEEE Trans. Reliab.* **2012**, *61*, 50–67.
108. Wang, X.; Balakrishnan, N.; Guo, B. Residual life estimation based on a generalized Wiener degradation process. *Reliab. Eng. Syst. Saf.* **2014**, *124*, 13–23.
109. Zhang, Z.X.; Si, X.S.; Hu, C.H. An age-and state-dependent nonlinear prognostic model for degrading systems. *IEEE Trans. Reliab.* **2015**, *64*, 1214–1228.
110. Liao, H.; Tian, Z. A framework for predicting the remaining useful life of a single unit under time-varying operating conditions. *Iie Trans.* **2013**, *45*, 964–980.
111. Liu, T.; Sun, Q.; Feng, J.; Pan, Z.; Huangpeng, Q. Residual life estimation under time-varying conditions based on a Wiener process. *J. Stat. Comput. Simul.* **2017**, *87*, 211–226.
112. Ye, Z.S.; Chen, N.; Shen, Y. A new class of Wiener process models for degradation analysis. *Reliab. Eng. Syst. Saf.* **2015**, *139*, 58–67.
113. Peng, C.Y.; Tseng, S.T. Statistical lifetime inference with skew-Wiener linear degradation models. *IEEE Trans. Reliab.* **2013**, *62*, 338–350.
114. Wen, Y.; Wu, J.; Das, D.; Tseng, T.L.B. Degradation modeling and RUL prediction using Wiener process subject to multiple change points and unit heterogeneity. *Reliab. Eng. Syst. Saf.* **2018**, *176*, 113–124.
115. Son, J.; Zhang, Y.; Sankavaram, C.; Zhou, S. RUL prediction for individual units based on condition monitoring signals with a change point. *IEEE Trans. Reliab.* **2014**, *64*, 182–196.
116. Gebraeel, N.Z.; Lawley, M.A.; Li, R.; Ryan, J.K. Residual-life distributions from component degradation signals: A Bayesian approach. *IiE Trans.* **2005**, *37*, 543–557.
117. Ng, T.S. An application of the EM algorithm to degradation modeling. *IEEE Trans. Reliab.* **2008**, *57*, 2–13.
118. Yan, W.a.; Song, B.w.; Duan, G.l.; Shi, Y.m. Real-time reliability evaluation of two-phase Wiener degradation process. *Commun. Stat.-Theory Methods* **2017**, *46*, 176–188.
119. Chen, N.; Tsui, K.L. Condition monitoring and remaining useful life prediction using degradation signals: Revisited. *IiE Trans.* **2013**, *45*, 939–952.
120. Wang, X.; Jiang, P.; Guo, B.; Cheng, Z. Real-time reliability evaluation for an individual product based on change-point gamma and Wiener process. *Qual. Reliab. Eng. Int.* **2014**, *30*, 513–525.
121. Ke, X.; Xu, Z. A model for degradation prediction with change point based on Wiener process. In Proceedings of the 2015 IEEE International Conference on Industrial Engineering and Engineering Management (IEEM), Singapore, 6–9 December 2015; IEEE: Piscataway, NJ, USA, 2015; pp. 986–990.
122. Zhang, J.X.; Hu, C.H.; He, X.; Si, X.S.; Liu, Y.; Zhou, D.H. A novel lifetime estimation method for two-phase degrading systems. *IEEE Trans. Reliab.* **2018**, *68*, 689–709.

123. Zhang, A.; Wang, Z.; Bao, R.; Liu, C.; Wu, Q.; Cao, S. A novel failure time estimation method for degradation analysis based on general nonlinear Wiener processes. *Reliab. Eng. Syst. Saf.* **2023**, *230*, 108913.
124. Ma, J.; Cai, L.; Liao, G.; Yin, H.; Si, X.; Zhang, P. A multi-phase Wiener process-based degradation model with imperfect maintenance activities. *Reliab. Eng. Syst. Saf.* **2023**, *232*, 109075.
125. Wang, Z.; Ta, Y.; Cai, W.; Li, Y. Research on a remaining useful life prediction method for degradation angle identification two-stage degradation process. *Mech. Syst. Signal Process.* **2023**, *184*, 109747.
126. Chen, Z.; Huang, X.; Liu, A.; Ma, Y.; Zhang, J.; Zhang, Q.; Wang, R.; Li, Z. Reliability-Oriented Multiobjective Optimization of Electrical Machines Considering Insulation Thermal Lifetime Prediction. *IEEE Trans. Transp. Electrif.* **2023**, *10*, 2264–2276.
127. *IEC 60034-18-41*; Rotating Electrical Machines—Part 18–41: Partial Discharge Free Electrical Insulation Systems (Type I) Used in Rotating Electrical Machines Fed from Voltage Converters—Qualification and Quality Control Tests. International Electrotechnical Commissio: Geneva, Switzerland, 2014.
128. Venkatesan, S.; Manickavasagam, K.; Tengenkai, N.; Vijayalakshmi, N. Health monitoring and prognosis of electric vehicle motor using intelligent-digital twin. *IET Electr. Power Appl.* **2019**, *13*, 1328–1335.
129. Wang, Q.; Jiao, W.; Zhang, Y. Deep learning-empowered digital twin for visualized weld joint growth monitoring and penetration control. *J. Manuf. Syst.* **2020**, *57*, 429–439.
130. Aivaliotis, P.; Georgoulias, K.; Arkouli, Z.; Makris, S. Methodology for enabling digital twin using advanced physics-based modelling in predictive maintenance. *Procedia Cirp* **2019**, *81*, 417–422.
131. Li, Y.; Li, M.; Yan, Z.; Li, R.; Tian, A.; Xu, X.; Zhang, H. Application of Life Cycle of Aeroengine Mainshaft Bearing Based on Digital Twin. *Processes* **2023**, *11*, 1768.
132. Xiong, M.; Wang, H.; Fu, Q.; Xu, Y. Digital twin–driven aero-engine intelligent predictive maintenance. *Int. J. Adv. Manuf. Technol.* **2021**, *114*, 3751–3761.